Supplementary Materials and Methods

Clinical samples

For the RNA N6-methyladenosine (m^6A)-seq and RNA-seq analyses, five pairs of HCC BM and primary tumor samples were obtained from HCC patients who had undergone hepatic resection at the Eastern Hepatobiliary Surgery Hospital (EHBH). 6 samples of HCC with BM (BM HCC), 13 of HCC with metastasis (non-bone), and 10 advanced-stage HCC samples who had undergone hepatic resection at the same hospital were analyzed by liquid chromatography-tandem mass spectrometry (LC-MS/MS), methylated RNA immunoprecipitation-quantitative reverse transcription-polymerase chain reaction (MeRIP-qPCR), and qRT-PCR (**Supplementary Table 1**). Samples were immediately frozen in liquid nitrogen. The 10 samples (5 HCC primary focus and 5 HCC BM focus tissues) were used for further verification of the RNA m^6A-seq data by MeRIP-qPCR analysis. Immunochemistry (IHC) was used to analyze 265 paired HCC and normal specimens from consecutive patients who had undergone hepatic resection at the EHBH; the clinical characteristics of this cohort are tabulated in **Supplementary Table 2**. These specimens were immediately frozen in liquid nitrogen, followed by formalin fixation, paraffin embedding, and pathological verification.

Ultra-high performance liquid chromatography-multiple-reaction monitoring-tandem mass spectrometry

Oligo dT magnetic beads were used to purify mRNA. Two hundred nanograms of mRNA were treated with nuclease P1 (0.5 U, Sigma-Aldrich, St. Louis, MO, USA) in a 25 μL of 10 mM NH_4OAc (pH = 5.3) for 1 h at 42 ℃ after which 3 μL of 1 M NH_4HCO_3 and 1 μL of 1 U/μL alkaline phosphatase (Sigma) were added with incubation for 2 h at 37 ℃. The solution was neutralized with 1 μl of 3 M HCl, made up to 50 μL and passed through a 0.22 μm filter (Millipore, Burlington, MA, USA). The samples (10 μl for each injection) were analyzed on a reverse-phase ultra-performance liquid chromatography (UHPLC) C18 column (Agilent Technologies, Santa Clara, CA, USA) with an Agilent 6410 QQQ triple-quadrupole LC mass spectrometer using a positive electrospray ionization mode and quantification using retention times and ion

mass transitions of 268.0 to 136.0 (A) and 282.1 to 150.0 (m^6A), with calculations relative to standards run in the same batches. Calibration curves were used to calculate the m^6A:A ratio.

IHC analysis

IHC was conducted according to a previously published protocol [1]. The sections were heated, followed by incubation with primary antibodies for 30 min and secondary antibodies for 1 h at room temperature (RT). Details of the antibodies are shown in **Supplementary Table 9**. The sections were then counterstained with hematoxylin, developed with diaminobenzidine, and examined by three blinded pathologists. The H-scores [2] for the staining in selected fields at 400x magnification for *METTL3*, *YTHDF1*, cytoplasmic *ANLN*, *KIF2C*, *MYBL2*, *HMGB2*, and *AURKA* were determined; staining intensities were scored as 0, 1, 2, or 3 for negative, weak, intermediate, and strong brown staining, respectively. Total cell numbers and numbers of stained cells in each field were counted and the average percentages of positive cells were determined. The H-score was determined as: (% of cells stained at intensity category 1 × 1) + (% of cells stained at intensity category 2 × 2) + (% of cells stained at intensity category 3 × 3). The H-scores ranged from 0-300, with 0 indicating negative staining in all cells and 300 representing 100% of cells showing strong staining. Median H-score values were applied as cut-offs to separate low- and high-expression groups. For nuclear *ANLN* staining, the percentage of cells showing moderate-to-strong nuclear staining was determined and the median percentage was used to separate low- and high-expression groups.

Stable Cell Line Construction

The *METTL3*, *ANLN*, *SP1*, *HMGB2*, and *KIF2C* expressing lentivirus vector *(LV-METTL3-GFP-PRO, termed as LV-METL3; LV-ANLN-GFP-PURO*, termed as *LV-METTL3; LV-METTL3-PURO, termed as LV-METTL3; LV-ANLN; LV-SP1-GFP-PURO*, termed as *LV-SP1*; *LV-HMGB2-GFP-PURO*, termed as *LV-HMGB2; and LV-KIF2C-GFP-PURO*, termed as *LV-KIF2C*) and their control vector (LV-GFP-PURO,

termed as LV-NC) were supplied by Shanghai Yuan zhi Biotechnology Co., Ltd. The *YTHDF1* expressing lentivirus vector (*LV-YTHDF1-FLAG-PURO, termed as LV-YTHDF1*) and its control vector (LV-FLAG-PURO, termed as LV-NC) were supplied by Shanghai Yuan zhi Biotechnology Co., Ltd. Lentiviruses knock down *METTL3 (#1, #2, #3, termed as METTL3-KD1, METTL3-KD2, METTL3-KD3); YTHDF1 (#1, #2, #3, termed as YTHDF1-KD1, YTHDF2-KD2, YTHDF3-KD3); ANLN (#1, #2, #3, termed as ANLN-KD1, ANLN-KD2, ANLN-KD3); KIF2C (#1, #2, #3, termed as KIF2C-KD1, KIF2C-KD2, KIF2C-KD3); MYBL2 (#1, #2, #3, termed as MYBL2-KD1, MYBL2-KD2, MYBL2-KD3); HMGB2(#1, #2, #3, termed as HMGB2-KD1, HMGB2-KD2, HMGB2-KD3); AURKA (#1, #2, #3, termed as AURKA-KD1, AURKA-KD2, AURKA-KD3)* or NC (termed as Negative control) were purchased from Shanghai Yuan zhi Biotechnology Co., Ltd. Cells were plated at 1×10^5 cells/well and were transfected with lentivirus, following the provided directions. Puromycin (3 μg/mL; Biosharp, Gunagzhou, China) and/or amplicillin (3 μg/ml; Biosharp) were used to select infected cells for at least one week, and the efficiency of transfection was assessed by qRT-PCR or western blotting. All the targeted sequences are shown in **Supplementary Table 10**.

RNA extraction, reverse transcription, and qRT-PCR

Total RNA was extracted from the frozen samples using TRIzol (Takara, Dalian, China), following the provided directions. The RNA quality was examined using a Nanodrop 2000 spectrophotometer and agarose gel electrophoresis. One to two micrograms of the RNA were used for reverse transcription to cDNA using random primers and M-MLV Reverse Transcriptase (Invitrogen, Waltham. MA, USA). RT-PCR was conducted by the Taqman assay or SYBR Green system in a Step One Plus system (Applied Biosystems, Waltham, MA, USA), the relative mRNA levels were determined according to the ΔΔCt values. The sequences of the primers are provided in **Supplementary Table 11**.

MeRIP-qPCR

Methylated RNA immunoprecipitation-qPCR was performed using an adaptation of a published method [3]. After denaturation of poly-A-purified RNA for 10 min at 70 °C, it was immediately cooled on ice and treated with an anti-m^6A antibody in 1 mL 50 mM Tris-HCl with 400 U of RNasin Plus RNase Inhibitor (Promega, Madison, WI, USA), 750 mM NaCl, and 0.5% (v/v) Igepal CA-630 (Sigma-Aldrich) for 2 h at 4 ℃. The solution was then incubated with washed Dynabeads Protein G (Invitrogen) for 2 h at 4 °C with gentle shaking. Two elutions of the m^6A RNA were performed with 6.7 mM N^6-methyladenosine 5′-monophosphate sodium salt at 4 °C, and the material was precipitated 5 μg glycogen and a one-tenth volume of 3 M sodium acetate in 2.5 volumes of 100% ethanol at −80 °C overnight. m^6A concentrations in the precipitate were measured by qPCR. Fragmented mRNA was probed directly with the anti-m^6A antibody and assessed in a similar manner.

Enzyme-linked immunosorbent assay

The levels of *RANK*L and *OPG* in culture supernatants obtained over 48 h were measured using the Human *RANKL* and *OPG* kits (both Ray Biotech), following the provided directions.

Osteoclast differentiation assays

Bone marrow cells (BMCs) were obtained from the femurs of four-week-old mice and grown in minimum essential medium (MEM) with 15% FBS and macrophage colony-stimulating factor (M-CSF) (50 ng/mL) for three days. Adherent cells were harvested, washed three times with PBS, and plated in 12-well plates with conditioned medium from treated HCC cells, *M-CSF* (25 ng/mL), and *RANKL* (100 ng/mL) for three days. The cells were stained using a tartrate-resistant acid phosphatase positive (TRAP) kit (Sigma Aldrich), according to directions, to analyze osteoclast and preosteoclast formation. TRAP-stained cells with a minimum of three nuclei were defined as osteoclasts. A minimum of nine fields per plate were evaluated and the mean osteoclast numbers were recorded.

CCK8 (Cell Counting Kit-8) assay

A CCK-8 kit (C0038, Beyotime Biotechnology, Shanghai) was used to measure proliferation, as described [4].

Animal models

All the mouse experiments which were performed according to the Naval Medical University's approved guidelines. The investigation complied with all applicable ethical regulations related to animal research. To investigate the influence of *ANLN* on HCC cell lines' BM ability, luciferase-labelled Huh7 ($1 \times 10^{7)}$ cells in 50 μL 1× PBS were injected into the left ventricles of four- to six-week-old female nude using a 100-μl Hamilton Microliter syringe as described previously [5]. The BMs were monitored by the IVIS@ Lumina II system (Caliper Life Sciences, Hopkinton, MA, USA) for 10 min after intraperitoneal injection of 4.0 mg of luciferin (Gold Biotech, St. Louis, MO, USA) in 50 μL of saline. The hindlimb organs were removed and fixed for histological examination. The investigators were not blinded.

RNA immunoprecipitation (RIP) assays

RIP assays were performed using a Magna RIP RNA-Binding Protein Immunoprecipitation Kit (17–700, Millipore), according to provided directions. Magnetic beads were coated with 5 μg of the appropriate antibodies and incubated with cell lysates overnight at 4 °C. After six washes, the complexed material was treated with proteinase K digestion buffer, followed by extraction of the RNA with phenol-chloroform. Interactions between *YTHDF1* and *ANLN* mRNA were assessed qPCR and expressed relative to the input. Details of the antibodies are provided in **Supplementary Table 9**.

Chromatin Immunoprecipitation (ChIP)

The Magna ChIP G Kit (17-611; Millipore) was used in accordance with the manufacturer's directions. After cross-linking of cells with 37% formaldehyde (Sigma F8775) solution (final concentration 1%) for 10 min and quenching with glycine, the PBS-washed cells were resuspended in lysis buffer with protease inhibitors and vortexed intermittently for 15 min at 4 °C. After centrifugation (800 g; 5 min), the

pelleted cells were resuspended in nuclei lysis buffer and sonicated with a Misonix S-4000 sonicator at 50% amplitude 15-s pulse with 90-s rest between each pulse (10 cycles). The size of the chromatin was assessed by electrophoresis and was immunoprecipitated with either 3 μg anti-TCF4 or 3 μg anti-IgG (Millipore 17-10109) overnight at 4 °C. ChIP fragments were examined using RT-PCR and the primers provided in **Supplementary Table 11**.

Luciferase activity report assay

Wild-type (WT) and mutant (Mut) *ANLN* bind peaks (shown in **Fig.5H**) were inserted into pGL3 luciferase reporter by BgIII digestion. Huh7 and MHCC-97H cells were seeded in 48-well plates and the adherent cells were co-transfected with pGL3-binding peak-WT and-Mut plasmids together with Renilla using Lipofectamine™ 2000 (Invitrogen) for 48 h. Firefly and Renilla activities were measured and firefly activity was normalized to that of Renilla.

Immunoprecipitation (IP) and LC-MS

The Dynabeads Co-Immunoprecipitation Kit (14321D, Thermo Fisher) was used for IP, following the provided directions. Proteins were separated on SDS-PAGE and the bands were digested with trypsin. The peptides were applied to an LC gradient for 2 h and were analyzed on a Q Exactive HF mass spectrometer (Thermo Fisher Scientific). The data were compared with the mouse database by MaxQuant (https://maxquant.org/). The intensity-based absolute-protein-quantification (iBAQ) intensity was used for inter-sample comparisons. The antibodies used are shown in **Supplementary Table 9**.

Western blotting (WB)

Cells were lysed in RIPA buffer with protease and phosphatase inhibitors, as well as DTT and benzonase (Sigma-Aldrich). Protein concentrations were measured using a BCA kit (Thermo Scientific Pierce, Loughborough, UK). WB was performed as previously described using NuPAGE@Novex 4-12% Bis-Tris protein gels (Novex, Life Technologies, Carlsbad, CA, USA). The antibodies used are shown in **Supplementary Table 9**.

Nuclear and cytoplasmic protein extraction

Cells were fractionated using a cytoplasmic and nuclear protein/RNA extraction kit (Thermo Fisher Scientific) according to the supplied protocol. The loading controls for the nuclear and cytoplasmic fractions were laminB1 and α-tubulin, respectively.

Immunofluorescence

Cells ($4x10^4$) were grown in confocal plates, fixed with 4% formaldehyde for 20 min, and permeabilized with 0.1% Triton X-100 for 20 min. The cells were blocked with 5% BSA in Tris-buffered saline with Tween 20 TBST) and were probed with the appropriate primary antibodies overnight at 4 °C. After incubation with secondary antibodies (30 min, RT) and nuclear staining with DAPI, the cells were examined and imaged with a confocal microscope (Olympus, Tokyo, Japan). The antibodies used are shown in **Supplementary Table 9**.

Patient-Derived Xenografts

For the patient-derived tumor xenograft (PDX) model, fresh tumor tissues were cut into 3x3 cm sections and implanted subcutaneously into the mouse flanks. The mice were given 3-deazaneplanocin A (DZNeP; 8 mg/kg per mouse) or dimethylsulfoxide (DMSO) orally 7 times for 2 weeks. The growth of the tumors was assessed at the indicated times. This procedure was approved by the EHBH Ethics Committee. Growth rates were calculated as previously described [6].

DZNeP treatment

Cells were treated with 10 μM DZNeP (Selleck, Houston, TX, USA; S7120) to prevent m^6A modification. Mice received subcutaneous injections of DZNeP (8 mg/kg) every other day.

m^6A-Seq

The m^6A-Seq method was used to measure m^6A RNA methylation. The library was constructed using the Next® Ultra™ II RNA Library Prep Kit (E7775; NEB), quantified with a Qubit Fluorometer (Thermo Fisher Scientific), and size distributions confirmed with Tape Station D1000 Screen Tape (Agilent Technologies). Sequencing

was done on an Illumina platform using PE150 (Shanghai OE Biotech, Shanghai, China).

Data processing and peak calling for m^{6}A-seq

We used Fast p v0.20.0 (https://github.com/OpenGene/fastp) was used to remove adapter and low-quality reads. Both MeRIP and input reads were aligned to the human genome (GRCh38.p12) using HISAT2 v2.1.0 (http://daehwankimlab.github.io/hisat2/) with parameter --rna-strandness RF --fr. The m6A peak calling was performed using the R package MeTDiff v 1.1.0. The P-value < 0.05 was set as the threshold for a significant m6A peak. We used MEME-ChIP v5.0.5 (https://meme-suite.org/meme/tools/meme-chip) to identify enriched motifs in the m6A peak region. The m^{6}A peak distribution on the metagene was plotted by R package Guitar v1.1.1.18. Analysis of differential m6A methylation was also performed using MeTDiff. Peak annotation was performed using ChIPseeker v1.12.1 (https://www.bioconductor.org/packages/release/bioc/vignettes/ChIPseeker/inst/doc/ChIPseeker.html).

RNA-Seq analysis

Total RNA was extracted using an ESciences RNA-Quick Purification Kit (Yi Shan Biotech, Shanghai, China). Library construction and RNA-seq were done by the OE Biotech company (Shanghai, China) with Illumina Nova Seq 6000 (Illumina, San Diego, CA, USA) and the data analyzed. Differentially expressed genes (DEGs) were analyzed by Gene Ontology (GO) annotation enrichment and Kyoto Encyclopedia of Genes and Genomes (KEGG) pathway enrichment with R based on the hypergeometric distribution. The criteria for differential genes were set up with P-value < 0.05 and fold change > 2 or < 0.5.

CUT&Tag library and sequencing

Huh7 cells were obtained from the American Type Culture Collection (ATCC; Manassas, VA, USA) and grown according to the supplier's protocol. We used the following antibodies: ANLN Primary antibody. A cleavage under targets and tagmentation (CUT&Tag) library was constructed using Hyperactive TM In-Situ ChIP

Library Prep Kit (TD901, Vazyme, Nanjing, China). In short, after harvesting, counting, and centrifugation (600 g; 3 min; RT), 60-500 000 cells aliquots were washed twice in 500 μL wash buffer by gentle pipetting. Ten microliters of prepared Concanavalin A-coated magnetic beads were added to each sample and incubated at RT for 10 min. Following the protocol, the cells were subjected to successive incubations with the beads, primary antibody, secondary antibody, and Hyperactive PG-TN5/PA-TN5 Transposon, and then fragmented. The fragmented DNA was isolated and amplified by PCR to obtain the library, which was sequenced using PE150 on the Illumina sequencer (Shanghai OE Biotech, China).

Data processing for CUT&Tag

We used Fastp v0.20.0 was used to remove adapter and low-quality reads. We then aligned paired-end reads using Bowtie2 version 2.3.4.3 (https://sourceforge.net/projects/bowtie-bio/files/bowtie2/2.3.4.3/) with options: -end-to-end-sensitive. Duplicated reads were removed using Picard v2.18.17 (https://github.com/nigyta/rice_reseq/blob/master/tools/picard-FastqToSam.cwl) with this parameter: REMOVE_DUPLICATES = true. For peak calling, SEACR v1.3 (https://github.com/FredHutch/SEACR) was used with threshold: 0.01. Scatterplots, correlation plots, and heatmaps were displayed using deep Tools v2.27.1 (https://deeptools.readthedocs.io/en/develop/). Annotation of peaks was performed using an R package ChIP seeker v1.12.1 and MEME ChIP v5.0.5 was used to search for the binding site.

Supplementary Figures

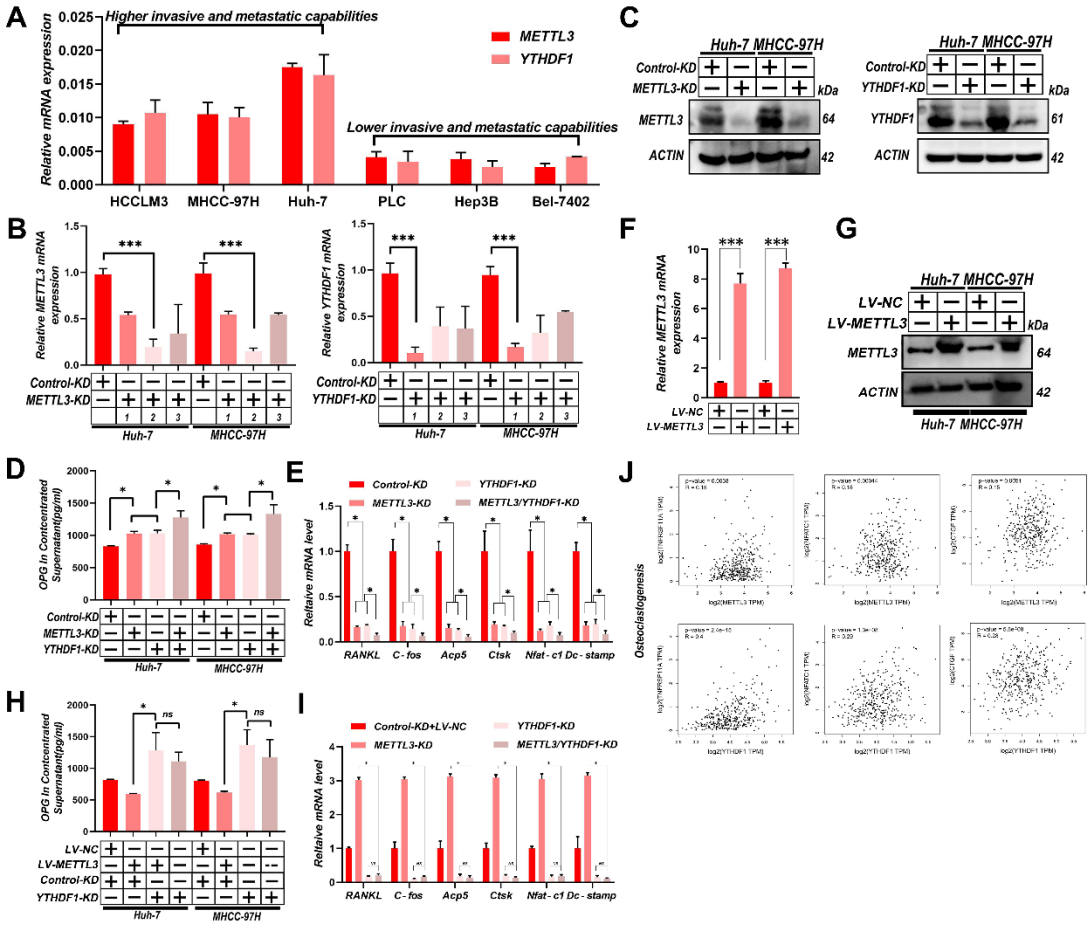

Supplementary Figure 1.

A. *METTL3* and *YTHDF1* mRNA levels in HCC cell lines were assessed using qRTPCR.

B&C. qRT-PCR and WB showed the *METTL3 and YTHDF1* mRNA (**B**) and protein (**C**) levels after silencing of *METTL3* and *YTHDF1*, respectively. *METTL3*-KD#2 and *YTHDF1*#1, which induced the most significant knock-down (KD) effect, respectively, was adopted for further study.

D. Concentration of *OPG* in the culture medium measured by ELISA from *METTL3/YTHDF1* knockdown and control HCC cell clones.

E. Osteoclastogenesis differentiation-related factors mRNA level of RAW264.7 cells with conditioned medium from (**D**) was measured by qRT-PCR treated.

F&G. qRT-PCR and WB measurement of *METTL3* mRNA and protein levels in HCC cells with LV-METTL3 or LV-NC.

H. Concentration of *OPG* in culture supernatants determined by ELISA from the *METTL3* overexpression and control HCC cells were infected with *YTHDF1*-KD or Control-KD HCC cell clones.

I. Osteoclastogenesis differentiation-related factors mRNA level of RAW264.7 cells with conditioned medium from (**H**) was determined by qRT-PCR.

J. Correlations of *METTL3 and YTHDF1* with several of osteoclastogenesis-related factors in HCC tissues based on GEPIA database. For (B&F) Paired t-test, (D&E, H&I) one-way ANOVA, (J) Pearson correlation analysis. Error bars represent means ± SD from three independent experiments, *$p < 0.05$; **$p < 0.01$; ***$p < 0.001$; NS $p > 0.05$.

qRT-PCR, quantitative reverse transcription-polymerase chain reaction; WB, western blot; HCC, hepatocellular carcinoma; mRNA, messenger RNA; ELISA, enzyme-linked immunosorbent assay; ANOVA, analysis of variance; SD, standard deviation; NS, not significant

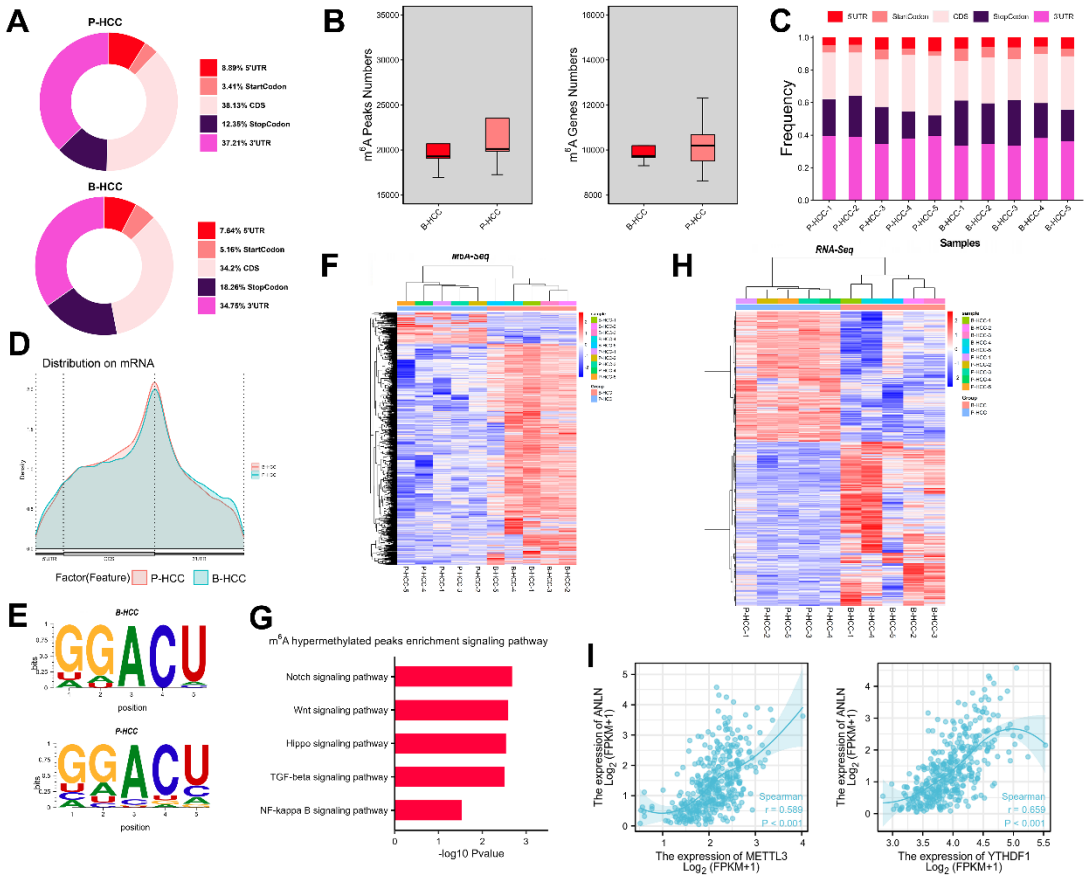

Supplementary Figure 2.

A- E. RNA categories (**A**), the methylation level change of differential m^{6}A sites in genes (**B**), mRNA region distributions (**C**), the distribution patterns ofm^{6}A methylation peaks in gene structures of mRNA (**D**), and logo plot (**E**) of m^{6}A sites in 5 B-HCC and 5 P-HCC samples.

F. Heatmap of changes in methylation levels of differential m^{6}A sites between 5 B-HCC and 5 P-HCC samples.

G. Canonical pathway analysis of hypermethylated mRNAs in B-HCC was shown (WNT, Hippo, Notch, TGF-β, and NF-κB).

H, Heatmap of differentially expressed mRNAs between 5 B-HCC and 5 P-HCC samples.

I, the correlation between *METTL3* and *YTHDF1* with *ANLN* in HCC tissues based on GEPIA database, respectively. For (I) Pearson correlation analysis.

M^6A, N6-methyladenosine; mRNA, messenger RNA; B-HCC, hepatocellular carcinoma bone metastasis focus; P-HCC, HCC primary focus; TGF-β, transforming growth factor-β; NF-κB, nuclear factor κB GEPIA, gene expression profile interactive analysis

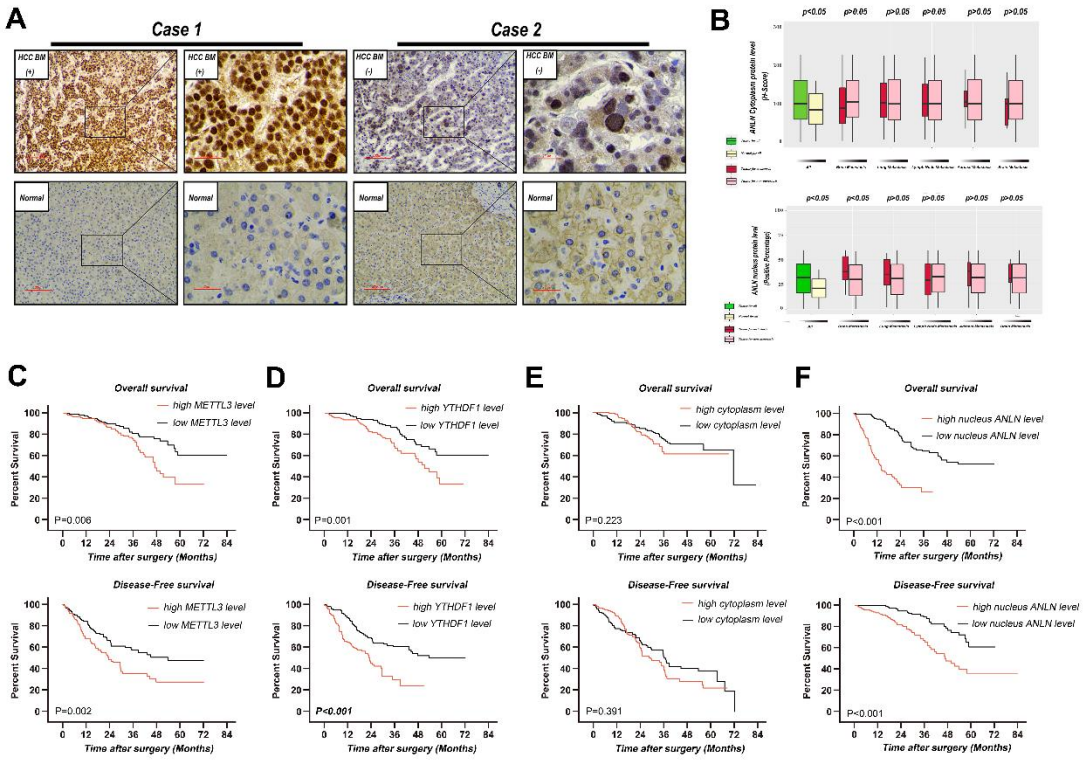

Supplementary Figure 3.

A. Images of representative *ANLN* staining are shown. Scale bar = 100 μm; Scale bar = 25μm.

B. IHC H-Scores of cytoplasm staining and relative nucleus expression of *ANLN* protein from 265 cases.

Of these 265 patients, there were 45 with BM, 53 with lung metastasis, 40 with LNM, 10 with adrenal gland metastasis, and 9 with brain metastases. Note： multiple organ metastases are represented in each relevant organ group.

C - F. Kaplan-Meier OS and DFS curves for 265 HCC patients expressing high or low levels of *METTL3* (**C**), *YTHDF1* (**D**), nucleus *ANLN* (**E**) and cytoplasm *ANLN* (**F**) stain. (B) Unpaired t-test, (C-F) log-rank test. Error bars represent means ± SD from three independent experiments, *p < 0.05; **p < 0.01; ***p < 0.001; NS p > 0.05.

HCC, hepatocellular carcinoma; mRNA, messenger RNA; OS, overall survival; DFS, disease-free survival; SEM, standard error of the mean; NS, not significant

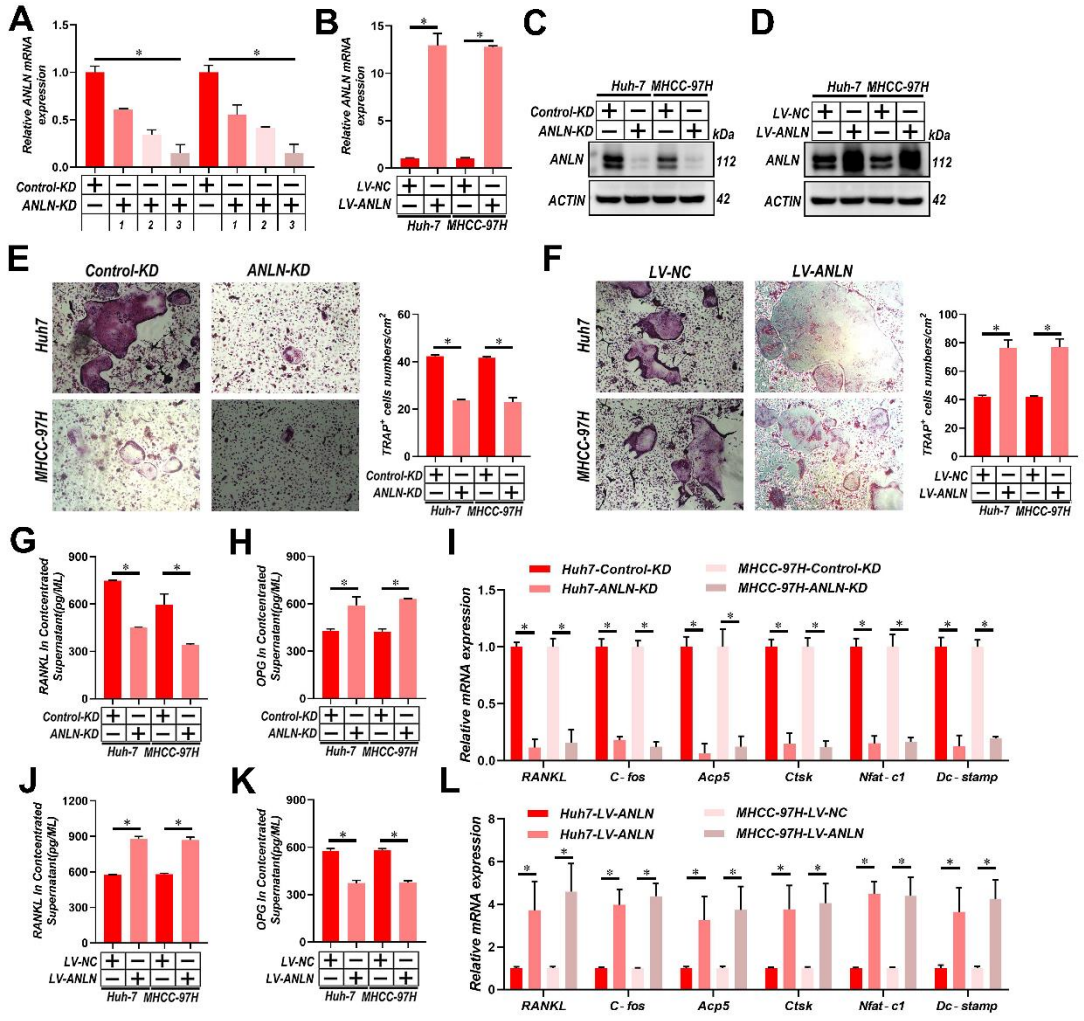

Supplementary Figure 4.

A&**B.** *ANLN* mRNA levels measured by qRT-PCR from indicated HCC cells. *ANLN*-KD#3 which induced the most significant knock-down (KD) effect, respectively, was adopted for further study.

C&**D**. Confirmation of *ANLN* knockdown (KD; *ANLN*-KD), and over-expression (LV-*ANLN*) in HCC cell lines were performed by WB.

E&F. Osteoclast differentiation assays were co-cultured with conditioned media from the HCC cells group in (**C&D**) containing M-CSF (25 ng/mL) and *RANKL* (100 ng/mL), magnification × 200.

G&J. Concentrations of *RANKL* in culture supernatants determined by ELISA from each group HCC cell.

H&K. Concentrations of *OPG* in culture supernatants determined by ELISA from each group HCC cell.

I&L. Osteoclastogenesis differentiation-related factors mRNA level of RAW264.7 cells with conditioned medium from (**F&G**) was measured by qRT-PCR treated.

For (A & B, G-L) Paired t-test. Error bars represent means ± SD from three independent experiments, *$p < 0.05$; **$p < 0.01$; ***$p < 0.001$; NS $p > 0.05$.

qRT-PCR, quantitative reverse transcription-polymerase chain reaction; WB, western blot; BLI, BLI, bioluminescence imaging; M-CSF, macrophage colony-stimulating factor; HCC, hepatocellular carcinoma; mRNA, messenger RNA; ELISA, enzyme-linked immunosorbent assay; SD, standard deviation

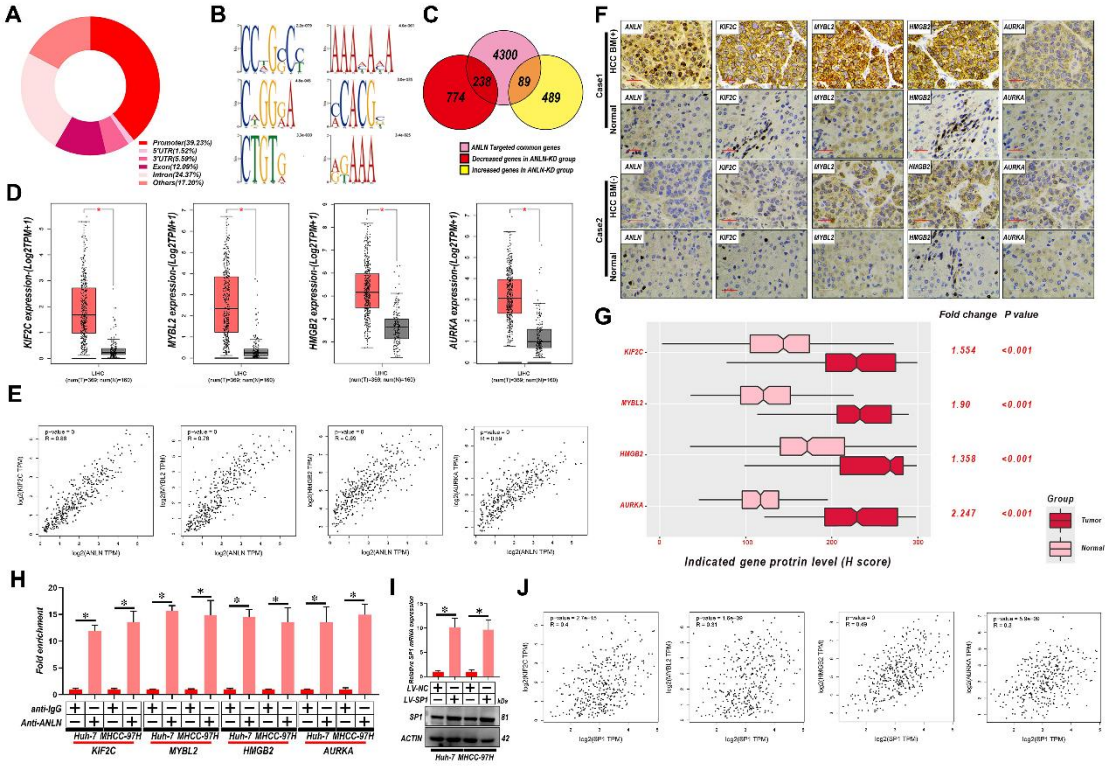

Supplementary Figure 5.

A. CUT&Tag seq dataset for *ANLN* in Huh7 cells produced using anti-ANLN antibody. The pie chart indicates the genome-wide distribution of ANLN occupancy in promoter, exon, intron, and intergenic regions in Huh7 cells after peak calling.

B. *ANLN*-binding consensus in Huh7 cells, Top 6.

C. Venn diagram of *ANLN*-regulated genes (Control vs. *ANLN*-KD: Blue circle, down-regulated; Green circle, up-regulated) and *ANLN*-targeted genes (Blue circle).

D. Expression of *KIF2C*, *MYBL2*, *HMGB2*, and *AURKA* transcript expression in HCC and normal tissues were performed in the GEPIA database.

E. The correlation between *ANLN* and *KIF2C*、*MYBL2*、*HMGB2*、and *AURKA* in HCC based on GEPIA database, respectively.

F. Representative IHC stains of *KIF2C*, *MYBL2*, *HMGB2*, and *AURKA* in matched 265 HCC and adjacent normal tissues. Scale bars, 200 μm, scale bars, 25 μm.

G. Histochemistry score (H-Score) was used to calculate the relative protein expression of *KIF2C*, *MYBL2*, *HMGB2*, and *AURKA* in 265 paired HCC and adjacent normal tissues.

H. Hun7 and MHCC-97H were harvested and analyzed by ChIP assays with an anti-ANLN antibody and qPCR. The figure shows ChIP-qPCR assessments of *ANLN* enrichment at the *KIF2C*, *MYBL2*, *HMGB2*, and *AURKA* promoter regions.

I. qRT-PCR and WB measurements of *SP1* mRNA and protein levels in HCC cells with LV-NC or LV-*SP1*.

J. The correlation between *SP1* and *KIF2C*、*MYBL2*、*HMGB2*、and *AURKA* in HCC based on GEPIA database, respectively,

For (D, G, and H & I) Paired t-test, (E, J) Pearson correlation analysis. Error bars represent means ± SD from three independent experiments, *p < 0.05; **p < 0.01; ***p < 0.001; NS p > 0.05.

CUT&Tag, cleavage under targets and tagmentation; HCC, hepatocellular carcinoma; GEPIA, gene expression profile interactive analysis; IHC, immunohistochemical; qRT-PCR, quantitative reverse transcription-polymerase chain reaction; WB, western blot; SD, standard deviation; NS, not significant

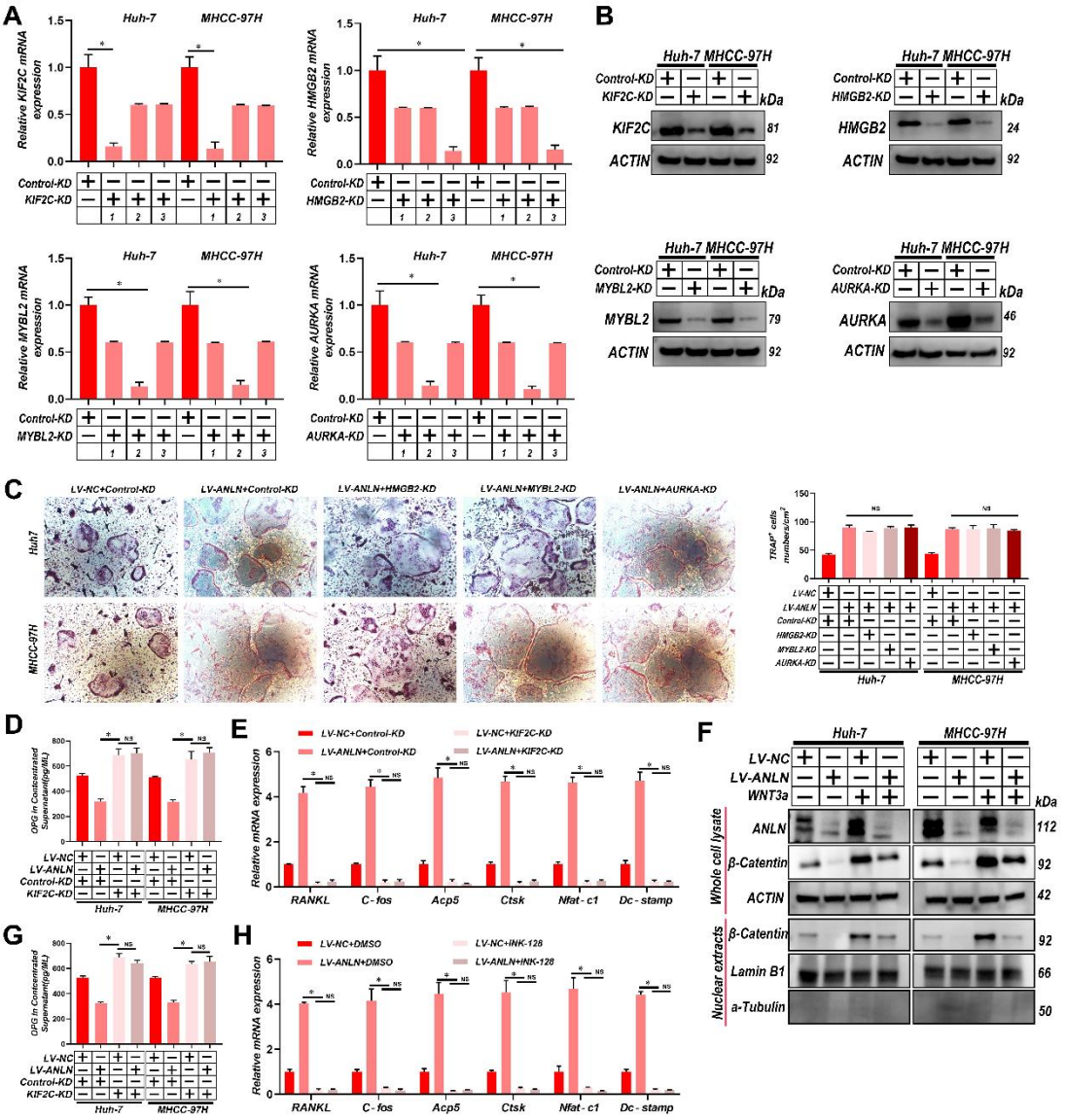

Supplementary Figure 6.

A&B. Confirmation of *KIF2C*, *HMGB2*, *MYBL2*, and *AURKA* knockdown (KD) in HCC cell lines were performed by qRT-PCR and WB. *KIF2C*-KD#1, HMGB2-KD#3, *MYBL2#2* and *AURKA#2*, which induced the most significant knock-down (KD) effect, respectively, was adopted for further study.

C. Osteoclast differentiation assays were co-cultured with conditioned media from the indicated HCC cells group containing M-CSF (50 ng/mL) and *RANKL* (100 ng/mL), magnification × 200.

D. Concentration of *OPG* in the culture medium measured by ELISA from each group HCC cell.

E. Osteoclastogenesis differentiation-related factor mRNA levels in RAW264.7 cells with conditioned medium from (**D**), determined by qRT-PCR.

F. WB showing levels of marker proteins (Lamin B1: nuclear marker, α-tubulin: cytoplasmic marker).

G. *ANLN* overexpression and control HCC cells were treated with or without INK-128, concentration of *OPG* in the culture medium measured by ELISA from each group HCC cell.

H. Osteoclastogenesis differentiation-related factors mRNA level of RAW264.7 cells with conditioned medium from (**G**), determined by qRT-PCR.

For (A) Paired t-test, (C-E, G&H) one-way ANOVA. Error bars represent means ± SD from three independent experiments, *$p < 0.05$; **$p < 0.01$; ***$p < 0.001$; NS $p > 0.05$.

HCC, hepatocellular carcinoma; qRT-PCR, quantitative reverse transcription-polymerase chain reaction; WB, western blot; M-CSF, macrophage colony-stimulating factor; ANOVA, analysis of variance; SD, standard deviation; NS, not significant

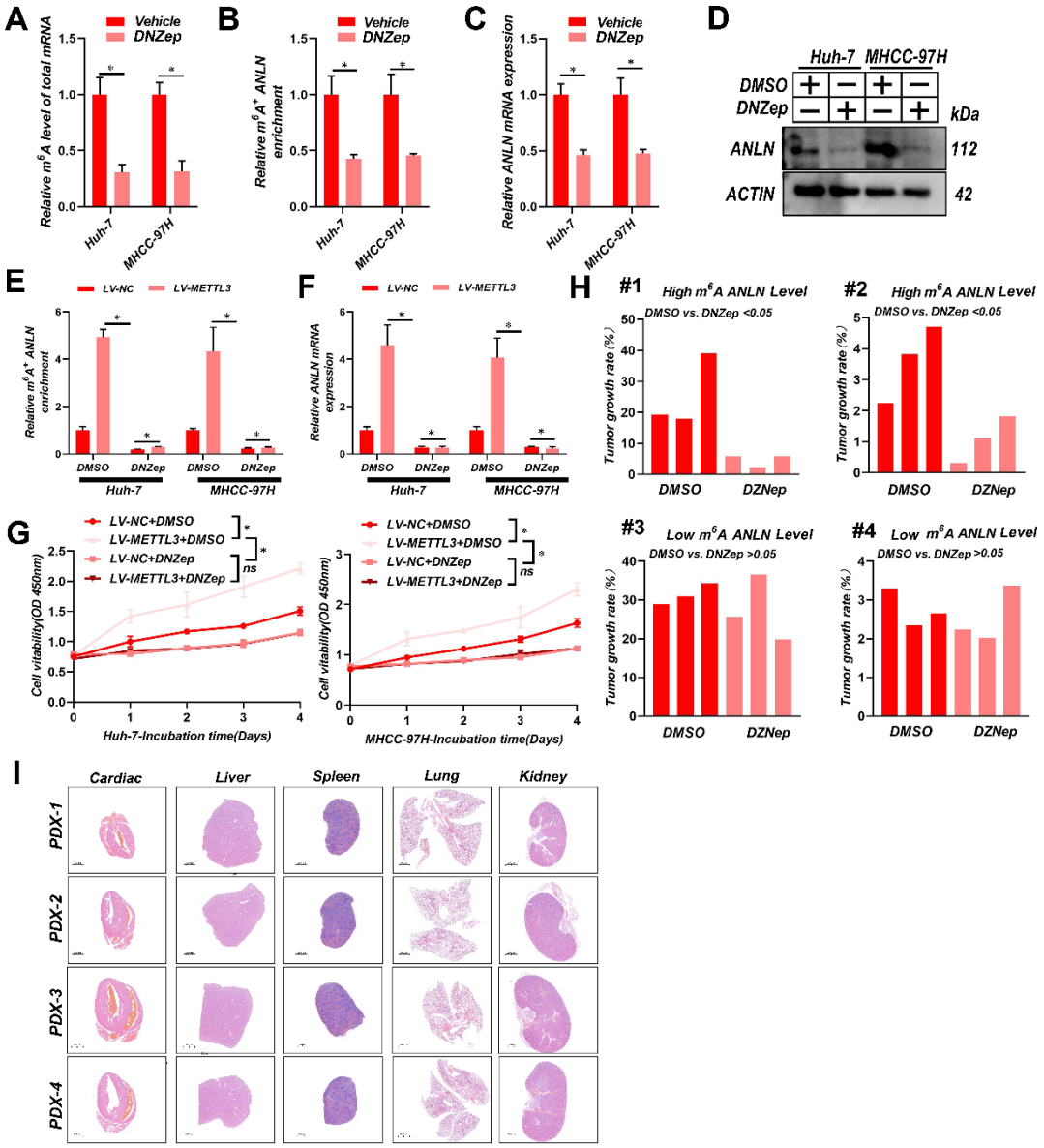

Supplementary Figure 7.

A. m^{6}A levels in HCC cells treated with vehicle or DZNep (10 mM) assessed using LC-MS/MS.

B. MeRIP-qPCR analysis was employed to assessment the *ANLN* m^{6}A modifications in HCC cells treated with vehicle or DZNep (10 mM).

C&D. *ANLN* mRNA and protein levels in HCC cells treated with vehicle or DZNep (10 mM), shown by qRT-PCR and WB, respectively.

E. MeRIP-qPCR assessment of *ANLN* m^{6}A modifications in HCC cells with *LV-NV or LV-METTL3*, and treated with vehicle or DZNep (10 mM).

F. *ANLN* mRNA levels determined by qRT-PCR in HCC cells with LV-NV or *LV-METTL3* and treated with vehicle or DZNep (10 mM).

G. The *in vitro* CCK8 assays in HCC cells with *LV-NV or LV-METTL3*, and treated with vehicle or DZNep (10 mM).

H. Growth of xenograft tumors. Vehicle (DMSO)-treated PDX were used as controls.

I. H&E staining of mice organs was performed from(**H**).

For (A-C, G, H) Paired t-test, (E and F) one-way ANOVA. Error bars represent means ± SD from three independent experiments, *$p < 0.05$; **$p < 0.01$; ***$p < 0.001$; NS $p > 0.05$.

M^6A, N6-methyladenosine; HCC, hepatocellular carcinoma; qRT-PCR, quantitative reverse transcription-polymerase chain reaction; WB, western blot; ANOVA, analysis of variance; SD, standard deviation; NS, not significant; MeRIP-qPCR, methylated RNA immunoprecipitation-quantitative reverse transcription-polymerase chain reaction; DZNep, 3-deazaneplanocin A; LC-MS/MS, liquid chromatography tandem mass spectrometry

Supplementary Tables

Table S1. Summary of clinico-pathologic characteristics of 29 HCC patients.

Group	Patient ID	Gender	Age	serum AFP, ng/mL	Tumor diameter, cm	Tumor number	Vascular invasion	TBIL, μmol/L	ALT, U/L	PT, s	PLT, 10^9/L
advantage-stage HCC	1	Male	42	1210	2.7	1	Presence	9.1	10.6	12.4	146
	2	Male	55	1210	4.8	1	Presence	16.6	48.8	13	109
	3	Male	46	70	4.8	2	Presence	10.9	113.3	12.8	154
	4	Male	41	1210	4.3	1	Presence	10.8	31.2	13.2	212
	5	Male	60	1210	5	2	Presence	18.6	44.5	12.2	195
	6	Male	42	2.3	4.2	1	Presence	15.6	33.3	11.6	100
	7	Male	50	2.1	4.9	1	Presence	13.4	20.2	12	175
	8	Male	37	14.1	2.8	1	Presence	19.6	18.5	10.7	82
	9	Male	60	1210	4	1	Presence	12.3	80.9	12.5	122
	10	Male	40	4.9	3.2	1	Absence	24	42.8	14.4	31
HCC with metastasis (non-bone)	1	Male	44	72.5	2.4	1	Absence	21.4	52	12.1	176
	2	Male	27	3.4	3.2	1	Absence	9.9	34.1	12	214
	3	Male	51	5.6	3.3	1	Absence	15.1	23.9	11	124
	4	Male	39	13.2	3.2	1	Absence	11.7	39.9	11.8	323
	5	Male	51	3.5	3.3	1	Absence	21.1	69.3	10.4	156
	6	Male	40	474	1.8	1	Absence	13.4	40.3	12.5	101
	7	Male	41	325	1.3	1	Absence	10.5	35.4	11.9	143
	8	Male	54	12.2	5	1	Absence	6	26.8	10.7	229
	9	Male	29	15.5	2.5	2	Absence	19	44	12.3	165
	10	Male	42	>1210	8	1	Presence	22.3	58	12.5	137
	11	Male	53	629.7	5	>3	Absence	2.4	22	10.9	186
	12	Male	48	9	11.6	1	Absence	13.1	44	12.7	216
	13	Female	53	49.4	8	1	Absence	12	42	10.6	141
HCC with BM	1	Male	64	143	11	2	Absence	3.8	16	11.5	287
	2	Male	66	3.6	10	1	Presence	11.5	45	10.6	173
	3	Male	29	53778	8.6	1	Absence	18.8	45	11.3	157
	4	Male	43	426	15.3	2	Absence	23.7	27	14.1	271
	5	Male	31	9992	8.9	1	Absence	13.7	43	11.4	126
	6	Male	67	4.6	10	>3	Absence	12.3	65	9.8	276

HCC, hepatocellular carcinoma; BM HCC, HCC with bone mestasis; TBIL, total bilirubin; ALT, alanine aminotransferase; PT, prothrombin time; PLT, platelet; HBeAg, hepatitis Be antigen

Table S2. Summary of clinico-pathologic characteristics IHC Cohort (n=265).

Clinico-pathologic characteristic		N
Gender	Female	35 (13.2%)
	Male	230 (86.8%)
Age, year	**≥55**	88 (33.2%)
	<55	177 (66.8%)
HBsAg	Negative	4 (1.51%)
	Positive	261 (98.5%)
HBV DNA, cpa/mL	≥ 1000	165 (62.3%)
	< 1000	100 (37.7%)
AFP, ng/mL	≥20	72 (27.2%)
	<20	193 (72.8%)
Vascular invasion	No	176 (66.4%)
	yes	89 (33.6%)
Tumor diameter, cm	≥5	47 (17.7%)
	<5	218 (82.3%)
Tumor number	Single	202 (76.2%)
	Multiple	63(21.5%)
Tumor Capsule	Absence	59 (22.3%)
	Presence	206 (77.7%)
Liver Cirrhosis	No	92 (34.7%)
	Yes	173 (65.3%)

TBIL, total bilirubin; ALT, alanine aminotransferase; PT, prothrombin time; PLT, platelet; HBeAg, hepatitis Be antigen; IHC Cohort, immunohistochemistry cohort

Table S3. m^6A and transcript level of m^6A regulate genes in 6 HCC with BM (BM HCC), 13 HCC with metastasis (non-bone), and 10 advantage-stage HCC, as assessed using qRT-PCR analysis

Group	Metastasis(bone+) vs. Metastasis(bone-)		Metastasis(bone-) vs. no-Metastasis		Metastasis(bone+) vs. non-Metastasis	
	Foldchange	**p-value**	**Foldchange**	**p-value**	**Foldchange**	**p-value**
m^6A	1.612266238	0.019906515	1.718952882	0.003597039	1.066171853	0.669931
METTL3	2.76697575	0.000150521	2.46075325	0.000663556	0.889329533	0.418831
METTL14	0.916997687	0.657353693	1.160382144	0.463178941	1.265414472	0.039536
WTAP	0.906814899	0.604690641	0.901006863	0.582367949	0.993595125	0.96176
KIAA1429	0.434563829	0.011346058	0.758315438	0.154132577	1.745003585	0.011057
ALKBH5	0.179233225	1.89781E-06	0.727066888	0.011890817	4.056540803	3.07E-08
FTO	0.546718462	0.055294424	1.296767645	0.226639943	2.371894761	0.002514
YTHDF1	2.588847529	2.34341E-09	2.717462261	2.65911E-07	1.049680304	0.66467
YTHDF2	3.54162141	0.044841223	1.621534816	0.326483722	0.457854149	0.000274
YTHDF3	0.580681912	0.15089313	0.868910808	0.344686312	1.496362794	0.137908

HCC, hepatocellular carcinoma; BM HCC, HCC with bone mestasis

Table S4. List of genes with a significant m6A hypermethylation and up-regulated expression levels in 5 B-HCC vs. 5 P-HCC samples.

Gene	m^6A Peak		mRNA	
	Diff.Log2.FC	p-value	log2FoldChange	p-value
GPC3	12.4572754	0.000211266	5.423352434	3.15133E-08
MAGEA6	11.45155631	0.001342733	10.53480235	0.000499434
TRIM71	10.9129911	5.68529E-06	9.077473284	2.94033E-09
MAGEA12	10.87022834	0.002055018	10.25435875	0.000703119
REG3A	10.70888244	0.0001944	9.420241988	9.38696E-08
MAFA	10.24393369	0.000829402	8.032313619	0.000451791
KREMEN2	9.5471569	0.000242909	7.923597321	9.69889E-08
NAA11	9.22316457	0.003552641	23.08525504	2.40693E-14
BPIFB2	8.883203746	0.000528499	8.471042175	0.000321221
MAGEA10	8.857325058	0.001377232	22.91360668	3.70325E-14
MEP1A	8.775497385	0.001471962	6.305677358	0.000259655
TICRR	8.672902978	0.000224039	4.257441837	3.87697E-06
COL11A1	8.586398697	0.000700843	6.294084535	4.29543E-08
C20orf204	8.531011937	0.000237157	5.821451323	4.38937E-12
CCR8	8.411682056	0.000213738	4.623170612	0.000246411
KCNF1	8.142172121	0.001363504	5.698712402	0.000248883
PRAME	7.925111921	0.000524497	7.152787107	7.40783E-05
NOTUM	7.895103408	0.003480605	4.552731018	0.000120146
ZIC2	7.886597017	0.002507065	8.359057073	9.83892E-09
GPC3	7.874970119	7.45213E-05	5.423352434	3.15133E-08
ZIC5	7.857448977	0.004005667	6.379082207	0.000801129
SLC22A31	7.561087301	0.000435186	5.133470547	4.48504E-05
COL11A1	7.55149037	0.002518633	6.294084535	4.29543E-08
NPFFR2	7.533877749	0.002838726	7.710536855	2.78447E-05
B4GALNT4	7.465075936	0.001080227	4.492440609	4.00515E-05
ZIC2	7.37341852	8.82512E-05	8.359057073	9.83892E-09
IGFBPL1	7.301867939	0.000369771	4.061134838	4.7178E-06
GABRQ	7.194718334	0.012052278	6.045089432	2.16471E-05
PITX1	7.081516843	0.000639509	8.557427502	3.17882E-09
SIX4	6.993405653	0.000268619	4.846512979	4.59561E-05
SPINK5	6.978431652	0.01400182	5.532768438	1.33822E-06
CA12	6.917707128	0.000864271	5.457372325	4.10032E-05
CRYBG2	6.83088253	0.002418559	5.109525054	9.24401E-09
MEP1A	6.808561422	0.016594478	6.305677358	0.000259655
C5orf46	6.808506248	0.009824018	6.118909628	1.82684E-05
MEP1A	6.78997516	0.00370127	6.305677358	0.000259655
PRAME	6.664013245	0.003650552	7.152787107	7.40783E-05
NKD1	6.513261563	0.004344455	4.919387484	1.75791E-05
CENPF	6.395071763	0.001157275	4.092018883	8.71647E-11
CCNO	6.215516109	0.004405498	4.496338689	0.00040676

CACNG4	6.193455658	0.000498446	5.42749299	7.04038E-05
CDC25C	6.179229261	0.002862171	4.576076152	5.93672E-10
NAA11	6.175244457	0.00644871	23.08525504	2.40693E-14
EXO1	6.137457843	0.000902958	4.130487664	2.96599E-10
NKD1	6.122121231	0.005873604	4.919387484	1.75791E-05
NKD1	6.02914564	0.004518617	4.919387484	1.75791E-05
E2F8	5.936927922	0.000510963	4.048552813	2.82265E-11
TOP2A	5.930908096	0.015241869	4.060501119	6.67813E-12
PPP2R2C	5.815300062	0.001435768	7.423797575	1.22335E-06
SLC22A11	5.7859506	0.003213869	4.031917208	8.58607E-05
HOXA13	5.783308637	0.002224118	5.063294181	0.00044068
HOXA10	5.743600955	0.005796136	6.969466403	3.3998E-07
PPP2R2C	5.681542246	0.002257948	7.423797575	1.22335E-06
HOXA13	5.623458111	0.007833321	5.063294181	0.00044068
NOTUM	5.621608789	0.002287596	4.552731018	0.000120146
KCNJ6	5.613499064	0.001400604	5.909640603	4.38419E-06
DEPDC1	5.477321024	0.000787312	4.659499665	1.29432E-06
CENPF	5.476089347	3.07184E-05	4.092018883	8.71647E-11
OTX1	5.461838165	0.006883836	5.008753683	0.00013086
TOP2A	5.448307794	0.004007511	4.060501119	6.67813E-12
DEPDC1	5.428245877	0.002354101	4.659499665	1.29432E-06
CCR8	5.356524967	0.000766031	4.623170612	0.000246411
CENPF	5.326259472	2.8E-05	4.092018883	8.71647E-11
GPC3	5.315422219	0.002418674	5.423352434	3.15133E-08
CENPF	5.30020122	0.000179541	4.092018883	8.71647E-11
NRCAM	5.288605795	0.004783961	4.346381187	2.48314E-05
SLC2A1	5.052946623	0.000780508	4.020640443	7.1024E-05
SFN	5.044340256	0.000396558	4.909022212	5.40845E-08
MUC13	4.984176502	0.001020376	5.559976908	1.56519E-14
HOXA13	4.908245774	0.016237031	5.063294181	0.00044068
CENPF	4.896819619	0.005721252	4.092018883	8.71647E-11
UBE2C	4.793578261	0.008115567	4.835442051	5.42776E-09
NXPH4	4.789619414	0.013010984	4.637854416	1.71746E-05
CENPF	4.753549882	0.000201064	4.092018883	8.71647E-11
EXO1	4.712761645	0.049561479	4.130487664	2.96599E-10
AUNIP	4.66709518	0.004316035	4.476846181	4.91798E-05
CENPF	4.663038328	0.003574309	4.092018883	8.71647E-11
UHRF1	4.648932259	0.000434374	4.110385646	1.72976E-12
PRRX1	4.617118659	0.007840701	4.357241279	2.93366E-07
CENPF	4.611657775	0.000131089	4.092018883	8.71647E-11
TOP2A	4.558414279	0.002101467	4.060501119	6.67813E-12
GINS1	4.51603461	0.004565491	4.184492563	3.70177E-10
TICRR	4.483040539	0.007871365	4.257441837	3.87697E-06
NKD1	4.470241507	0.035929067	4.919387484	1.75791E-05

CENPF	4.434391484	0.017796527	4.092018883	8.71647E-11
ZBED2	4.357261373	0.004217319	6.592973596	1.04118E-05
MELK	4.342726821	0.004113781	4.184462107	1.1564E-10
GP2	4.314249193	0.045398181	5.559266596	2.33484E-05
EXO1	4.313968336	0.003942195	4.130487664	2.96599E-10
NCAPG	4.182223475	0.00611603	4.037536103	1.77113E-09
KIF15	4.130441334	0.016572759	4.209217227	8.43226E-10
EBF2	4.056045632	0.036089438	4.336271729	6.55617E-06
NEK2	4.031420154	0.010663666	4.891126562	1.27471E-09
TICRR	3.982143633	0.02073617	4.257441837	3.87697E-06
TOP2A	3.887706419	0.013359524	4.060501119	6.67813E-12
CENPA	3.885426596	0.003040713	5.027462865	2.01019E-07
GINS1	3.876862692	0.031751657	4.184492563	3.70177E-10
MYBL2	3.854692021	0.031707992	5.379512273	4.48175E-10
HS6ST2	3.84475521	0.028364567	4.622128617	0.000544563
TICRR	3.818082815	0.017431726	4.257441837	3.87697E-06
SIX4	3.794612887	0.01976303	4.846512979	4.59561E-05
MUC13	3.782292079	0.017404635	5.559976908	1.56519E-14
TOP2A	3.731049918	0.00652102	4.060501119	6.67813E-12
TOP2A	3.721243086	0.025913883	4.060501119	6.67813E-12
ANLN	3.714875427	0.015496257	4.129812832	6.56595E-09
SLC9A3	3.618003837	0.029739498	4.440875171	0.000501284
RHBDL3	3.468209427	0.037252031	4.19325615	0.000288592
TOP2A	3.368723298	0.019055311	4.060501119	6.67813E-12
CENPF	3.196553013	0.038648494	4.092018883	8.71647E-11

M^6A, N6-methyladenosine; HCC, hepatocellular carcinoma

Table S5. m^{6}A and transcript level of 68 genes in 6 HCC with BM (BM HCC), 13 HCC with metastasis (non-bone), and 10 advantage-stage HCC, as assessed using MeRIP-PCR analysis

Group	Metastasis(bone+) vs. Metastasis(bone-)		Metastasis(bone-) vs. no-Metastasis		Metastasis(bone+) vs. non-Metastasis	
MeRIP-PCR	**Foldchange**	**p-value**	**Foldchange**	**p-value**	**Foldchange**	**p-value**
ANLN	4.41097119	6.9589E-08	1.00578077	0.98084249	4.43647	3.0587E-08
GP2	1.11520815	0.20155093	2.61502154	6.8589E-05	2.91629333	3.5986E-07
NKD1	1.23510136	0.36843225	2.35671077	0.00493217	2.91077667	2.7247E-06
OTX1	1.39898955	0.22272577	1.99309923	0.00635125	2.788325	4.355E-05
EXO1	1.23188751	0.46290236	2.06489769	0.01183743	2.54372167	5.5243E-05
PRAME	1.19344668	0.08479948	1.08056077	0.28264937	1.28959167	0.0001035
CA12	1.21506517	0.03034816	1.05525615	0.53594539	1.282205	0.00013485
KIF15	1.10603128	0.87659103	2.64722923	5.3948E-05	2.92791833	0.00015582
MUC13	0.99901214	0.80093964	2.16941308	0.00391144	2.16727	0.00034175
NEK2	1.12636041	0.5217231	2.70688077	0.00049488	3.04892333	0.00037442
MELK	1.15475851	0.7904497	2.16800308	0.00530343	2.50352	0.00041439
GABRQ	1.09308751	0.17976759	1.20845615	0.00634012	1.32094833	0.00044973
SFN	1.32418518	0.29430388	1.70929769	0.02715035	2.26342667	0.00058316
UHRF1	1.2511435	0.33011492	2.20213615	0.00303816	2.75518833	0.0005843
SLC22A11	0.86229375	0.63256601	2.85834923	0.00018508	2.46473667	0.00123287
CDC25C	0.77422974	0.27126502	3.14545308	4.4226E-07	2.43530333	0.00130513
C5orf46	1.13325666	0.34883351	2.38719385	8.0531E-05	2.70530333	0.00139899
KCNJ6	1.11006919	0.99002977	2.76239538	9.6553E-05	3.06645	0.00144935
GINS1	1.22347386	0.38046447	2.04030923	0.00186591	2.496265	0.00158622
CRYBG2	0.87982795	0.42336493	2.53855692	0.00170111	2.23349333	0.00163699
PPP2R2C	1.05732595	0.7293931	2.41556385	0.00030013	2.55403833	0.0017587
MYBL2	0.95757277	0.8429739	2.22822231	0.01286456	2.133685	0.00201165
EBF2	0.96632733	0.80095664	2.30179077	0.00745297	2.22428333	0.00239525
B4GALNT4	1.24335247	0.20917048	1.05337923	0.58061599	1.30972167	0.00254544
NXPH4	0.94644147	0.76776834	2.41203154	0.00350878	2.28284667	0.00329343
CENPF	1.04412691	0.98854534	2.20308308	0.00658887	2.30029833	0.00443792
HOXA13	0.78497387	0.30292642	2.86614	1.952E-05	2.249845	0.00577499
CACNG4	1.12896581	0.55405943	2.08590462	0.00904615	2.354915	0.00609705
CENPA	0.98227278	0.94630536	2.39298769	0.00852236	2.35056667	0.00761244
HOXA10	0.87901953	0.4425548	2.37270231	0.00103784	2.08565167	0.010384
E2F8	1.04828849	0.81023706	2.30148	0.00108915	2.412615	0.01102018
CCNO	0.80037841	0.3352244	2.65511077	0.00019295	2.12509333	0.01723908
MAFA	1.10325965	0.665832	1.06362692	0.40312763	1.17345667	0.01785996
HS6ST2	0.72725138	0.2200008	2.65905077	3.7167E-05	1.93379833	0.01888521
TOP2A	0.96470821	0.90128788	2.02115	0.01381117	1.94982	0.02115081
PRRX1	1.03276068	0.6640342	2.25223846	0.02141728	2.32602333	0.02547686
SPINK5	1.0340706	0.38024536	1.06884385	0.33429036	1.10526	0.03141308

SLC22A31	1.02454345	0.73391712	1.15725692	0.01531797	1.18566	0.03426916
NCAPG	0.57719785	0.08295839	2.53900231	0.00018902	1.46550667	0.03476539
ZBED2	0.80048409	0.5403893	2.70488615	0.00065064	2.16521833	0.03835975
SLC2A1	0.79434238	0.47706038	2.82076308	0.00030008	2.24065167	0.04048174
DEPDC1	0.71294939	0.17442679	2.81994769	7.643E-05	2.01048	0.041575
NRCAM	0.76998298	0.44103905	2.52459692	0.00099161	1.94389667	0.04371602
C20orf204	1.06131875	0.5409399	1.12872154	0.14654624	1.19793333	0.05111414
NOTUM	1.03677415	0.64011742	1.14669462	0.10001068	1.18886333	0.0579736
IGFBPL1	1.09474503	0.60474101	1.08609308	0.31044501	1.188995	0.08329436
UBE2C	0.76821389	0.25222404	1.82148923	0.0345552	1.39929333	0.12095767
BPIFB2	1.20305392	0.11193887	0.95102692	0.39349666	1.14413667	0.12095804
ZIC5	0.96690204	0.54986683	1.15998308	0.05072419	1.12159	0.20251785
MAGEA10	0.91807455	0.21413943	1.15553615	0.02871957	1.06086833	0.22290894
SIX4	0.96793062	0.86602113	1.12248231	0.06287446	1.086485	0.24794827
ZIC2	1.00635073	0.83053268	1.09321231	0.2981986	1.100155	0.26538049
AUNIP	0.67776626	0.18864565	2.04648231	0.02099023	1.38703667	0.2839701
TICRR	0.8603772	0.21265855	1.08329231	0.23532104	0.93204	0.32514026
KCNF1	1.05775139	0.94491268	1.02354077	0.79118716	1.08265167	0.3270386
COL11A1	0.85172968	0.00453561	1.22612846	0.00159561	1.04433	0.33243582
CCR8	1.03154589	0.88878498	1.04449385	0.52272134	1.07744333	0.37825244
GPC3	0.99254625	0.95323082	1.07894385	0.39788712	1.07090167	0.41642794
NPFFR2	0.87991288	0.39245284	1.06581385	0.48813422	0.93782333	0.42153137
NAA11	0.99606062	0.94237537	1.06147154	0.47280677	1.05729	0.54634471
PITX1	0.99874162	0.86291518	1.04040923	0.5804665	1.0391	0.59181755
MEP1A	0.99583584	0.96897681	1.03551538	0.63826195	1.03120333	0.62062074
MAGEA12	0.94950841	0.82657897	1.06938846	0.4521716	1.01539333	0.84871221
REG3A	0.92636717	0.49295813	1.06071692	0.46714399	0.98261333	0.85992963
KREMEN2	0.94434126	0.62830017	1.07225538	0.45595069	1.012575	0.91903906
MAGEA6	0.93180212	0.68853294	1.08055846	0.30639057	1.00686667	0.93938049
TRIM71	0.93833941	0.5899775	1.06918846	0.37938573	1.00326167	0.9557742
SLC9A3	0.28829873	5.1639E-05	3.46554308	6.3312E-08	0.99911167	0.98265344

HCC, hepatocellular carcinoma; BM HCC, HCC with bone mestasis

Table S6. m^{6}A and transcript level of 68 genes in 6 HCC with BM (BM HCC), 13 HCC with metastasis (non-bone), and 10 advantage-stage HCC, as assessed using qRT-PCR analysis

Group	Metastasis(bone+) vs. Metastasis(bone-)		Metastasis(bone-) vs. no-Metastasis		Metastasis(bone+) vs. non-Metastasis	
qRT-PCR	Foldchange	p-vaule	Foldchange	p-vaule	Foldchange	p-vaule
ANLN	4.45799924	0.00028511	0.98927077	0.94952835	4.41016833	0.00028633
SFN	1.10154115	0.4617522	2.67577385	0.0013056	2.947475	5.9502E-11
C5orf46	1.58131456	0.02419206	2.19074692	0.00464888	3.46426	1.493E-06
NEK2	1.29120705	0.49716443	1.97912231	0.03597505	2.55545667	4.799E-06
NCAPG	1.19007236	0.46015225	2.50851692	0.00043333	2.98531667	3.114E-05
KCNJ6	1.29535481	0.38570583	2.31085077	0.00302023	2.99337167	6.2713E-05
SLC22A11	1.16922359	0.57008517	2.85464077	0.00123025	3.33771333	6.6387E-05
UBE2C	1.16566487	0.49766389	2.68875308	0.00017063	3.134185	6.6712E-05
CCNO	1.08802888	0.99783159	2.47042615	0.00037513	2.687895	7.3908E-05
MUC13	1.04485333	0.51786447	2.67675846	0.00024327	2.79682	0.00011042
CDC25C	1.46657546	0.22845257	1.77393077	0.04073805	2.60160333	0.0003606
CENPF	1.18166291	0.63527	2.59761615	0.0018171	3.06950667	0.00040994
ZBED2	0.81766425	0.39103	2.65983462	0.00017317	2.17485167	0.00045124
EBF2	1.07436872	0.41941612	2.59241538	0.00011239	2.78521	0.00060806
NKD1	1.04666475	0.7655985	2.74194769	0.00015598	2.8699	0.00085506
SLC2A1	0.93772885	0.47625525	2.18087385	0.01528809	2.04506833	0.00122641
GP2	1.44549101	0.03349208	1.64506615	0.02728607	2.37792833	0.00128756
PPP2R2C	0.72196821	0.33792805	3.18877385	7.6745E-06	2.30219333	0.00146162
NRCAM	1.28862366	0.55791053	1.90137231	0.05087376	2.45015333	0.00157
MYBL2	1.28100522	0.49816346	1.93432077	0.01827349	2.477875	0.0017065
NXPH4	0.9881801	0.9593101	2.77047	0.00014769	2.73772333	0.00194947
EXO1	1.04633886	0.64396244	2.03393	0.02172386	2.12818	0.00221534
GABRQ	1.11172141	0.50764558	1.11393615	0.2027629	1.23838667	0.00418726
PRRX1	0.93340987	0.92050729	2.27227615	0.01050742	2.120965	0.00494784
UHRF1	0.89660519	0.6440522	2.66035154	0.00021422	2.385285	0.00753053
DEPDC1	1.02444015	0.95484424	2.29797385	0.00306156	2.35413667	0.00825405
HOXA13	0.87980904	0.30132882	2.54984308	0.00245012	2.243375	0.01027168
CACNG4	1.07858113	0.93869853	2.2095	0.01384237	2.383125	0.0122228
MELK	0.95055752	0.85293505	2.40184308	0.00160634	2.28309	0.01843884
CRYBG2	0.82676577	0.63201474	2.68936308	0.00018324	2.22347333	0.02038293
SPINK5	1.07403202	0.49103061	1.13720538	0.10852529	1.221395	0.02224495
TICRR	1.07629248	0.26185231	1.07953308	0.26456885	1.16189333	0.03148091
HS6ST2	0.96788771	0.8376501	2.32679538	0.00398118	2.25207667	0.03510196
TRIM71	0.880229	0.03239603	1.02298	0.72272453	0.90045667	0.03601479
IGFBPL1	1.04727816	0.8043438	1.10446462	0.2005266	1.15668167	0.03633978
CA12	1.09524425	0.46186077	1.08101154	0.35716485	1.18397167	0.03884897
PITX1	1.09526409	0.32149353	1.09367231	0.28610328	1.19786	0.04605858

REG3A	1.18678385	0.04642721	0.98158846	0.82133396	1.16493333	0.04740807
HOXA10	0.58384835	0.02835469	3.08751692	5.6223E-06	1.80264167	0.05224957
E2F8	0.74579361	0.32899377	2.67438154	7.3488E-05	1.99453667	0.05563304
KIF15	0.64892629	0.180331	2.43578769	0.00087718	1.58064667	0.05656971
AUNIP	0.68693738	0.11407983	2.44790385	0.00028648	1.68155667	0.05962061
GINS1	0.84682113	0.55608483	2.16485308	0.00353303	1.83324333	0.08470484
COL11A1	1.1182519	0.5022626	1.02774846	0.7543766	1.14928167	0.09136707
TOP2A	0.67236628	0.30713331	2.90163769	9.1905E-05	1.95096333	0.10130106
SLC9A3	0.30749919	0.00010015	3.44191154	1.5428E-07	1.058385	0.10254363
ZIC5	1.05339675	0.74189302	1.11368769	0.26848925	1.173155	0.10517722
CENPA	0.75467941	0.49912776	2.31328692	0.01497755	1.74579	0.10571529
NAA11	0.99482784	0.92524126	1.16489	0.06156614	1.158865	0.13337587
B4GALNT4	1.02028452	0.74460195	1.09386154	0.27335038	1.11605	0.15507576
OTX1	0.73176816	0.48516841	1.95621385	0.0223581	1.431495	0.20228238
SIX4	1.02865692	0.62260386	1.11705692	0.15003839	1.14906833	0.2061045
PRAME	0.98358445	0.61182817	1.13489154	0.09945979	1.11626167	0.20626853
NOTUM	0.81844445	0.06743796	1.14501154	0.11507842	0.93712833	0.27178292
KCNF1	0.81345097	0.1271357	1.14072231	0.12340461	0.92792167	0.35368213
CCR8	0.98500473	0.4932481	1.07151769	0.34671661	1.05545	0.35916626
NPFFR2	0.98496154	0.85254367	1.08016231	0.38714971	1.06391833	0.3796466
C20orf204	0.97880671	0.90123202	1.08479538	0.27217329	1.061805	0.41201987
MAGEA6	0.97845846	0.88054508	1.09126077	0.32578749	1.06775333	0.42457349
MAGEA12	0.99828898	0.81690634	1.07200923	0.37366828	1.070175	0.42652201
SLC22A31	0.92642259	0.98877706	1.14292154	0.14057421	1.05882833	0.45139647
MAGEA10	1.03655862	0.62234112	1.02439615	0.78765034	1.06184667	0.5448025
MEP1A	0.92529375	0.35763923	1.13531154	0.14169459	1.05049667	0.62052395
MAFA	1.0265657	0.57644566	1.00631	0.93239014	1.03304333	0.62428241
KREMEN2	0.88032697	0.5379879	1.12120462	0.11246363	0.98702667	0.87954951
GPC3	0.94608064	0.62293466	1.06059846	0.41938799	1.00341167	0.96698655
BPIFB2	0.85927347	0.06434619	1.16607231	0.04403666	1.001975	0.97407384
ZIC2	1.0742991	0.67686375	0.93348615	0.15569744	1.00284333	0.97470409

HCC, hepatocellular carcinoma; BM HCC, HCC with bone mestasis

Table S7. The expression of 238 genes in HCC and normal tissues and Correlation coefficient(R) with ANLN expression in HCC based on GEPIA data.

Gene Name	UP/Down (LIHC/Normal)	Fold change（> 2/＜0.5）	p-Value	DFS- p-Value	OS- p-Value	R	p-Value
KIF2C	UP	YES	YES	6.20E-06	1.10E-05	0.86	0
CENPA	UP	YES	YES	0.0047	0.00078	0.86	0
PRR11	UP	YES	YES	0.011	0.0063	0.85	0
GTSE1	NO	NO	NO	0.0059	0.028	0.85	0
DLGAP5	UP	YES	YES	0.0033	0.00039	0.82	0
NCAPH	UP	YES	YES	0.00019	0.02	0.78	0
PHF19	UP	YES	YES	6.80E-05	0.0025	0.76	0
MYBL2	UP	YES	YES	0.0047	0.0034	0.76	0
BIRC5	UP	YES	YES	0.002	6.70E-05	0.76	0
CDCA3	UP	YES	YES	0.0017	0.00071	0.76	0
STIL	NO	NO	NO	0.0069	0.013	0.75	0
CDCA5	UP	YES	YES	0.00014	0.00021	0.75	0
HMGB2	UP	YES	YES	0.00044	0.0039	0.69	0
TACC3	UP	YES	YES	0.00021	0.0028	0.67	0
PIF1	NO	NO	NO	0.02	0.005	0.67	0
CBX5	NO	NO	NO	0.077	0.037	0.65	0
FAM83D	UP	YES	YES	0.011	0.0042	0.64	0
EME1	NO	NO	NO	7.80E-05	0.0029	0.63	0
IQGAP3	UP	YES	YES	0.058	0.00064	0.62	0
CNTNAP1	NO	NO	NO	0.24	0.0017	0.62	0
SAPCD2	NO	NO	NO	0.14	0.017	0.61	0
AURKA	UP	YES	YES	0.0012	0.00022	0.59	0
ARHGAP33	NO	NO	NO	0.0028	0.17	0.57	0
TRIM65	NO	NO	NO	0.0032	0.014	0.56	0
CARD19	NO	NO	NO	0.0047	0.034	0.49	0
ARHGAP22	NO	NO	NO	0.27	0.041	0.49	0
UAP1L1	NO	NO	NO	0.65	0.045	0.47	0
SH3BP1	NO	NO	NO	0.81	0.81	0.47	0
PAQR4	UP	YES	YES	0.0089	0.0088	0.47	0
PIK3R2	UP	YES	YES	0.16	0.094	0.46	0
RMI2	UP	YES	YES	0.0021	0.00082	0.44	0
LRRK1	NO	NO	NO	0.22	0.96	0.44	0
ITPKA	UP	YES	YES	0.094	0.41	0.44	0
PKMYT1	UP	YES	YES	0.0037	0.0017	0.42	0
IFI30	UP	YES	YES	0.58	0.15	0.42	0
TRIM47	NO	NO	NO	0.051	0.39	0.41	0
PLAU	UP	YES	YES	0.7	0.18	0.41	4.40E-16
FBLN1	UP	YES	YES	0.76	0.83	0.41	4.40E-16
PKN3	NO	NO	NO	0.014	0.1	0.4	1.30E-15

NLRC5	NO	NO	NO	1	0.87	0.4	8.90E-16
SYNGR2	UP	YES	YES	0.0025	0.053	0.38	7.00E-14
RAP1GAP	NO	NO	NO	0.59	0.014	0.38	5.30E-14
CHRM4	NO	NO	NO	0.43	0.35	0.38	7.20E-14
ZNF580	NO	NO	NO	0.0086	0.0012	0.37	2.70E-03
ZNF514	NO	NO	NO	0.008	0.15	0.37	3.50E-13
NSMF	NO	NO	NO	0.035	0.33	0.37	2.40E-13
MGAT5B	NO	NO	NO	0.6	0.027	0.37	2.50E-13
CAPG	UP	YES	YES	0.28	0.00045	0.37	4.40E-13
PLB1	NO	NO	NO	0.6	0.78	0.36	1.50E-12
PDZD7	NO	NO	NO	0.63	0.14	0.36	6.00E-13
UNC5B	NO	NO	NO	0.09	0.018	0.34	1.30E-11
TOX2	NO	NO	NO	0.67	0.76	0.32	4.70E-10
ENTPD2	NO	NO	NO	0.39	0.85	0.32	3.60E-10
ADM2	UP	YES	YES	0.87	0.11	0.32	1.90E-10
TLDC2	NO	NO	NO	0.086	0.28	0.31	1.10E-09
SYNC	NO	NO	NO	0.093	0.96	0.31	1.00E-09
RINL	NO	NO	NO	0.63	0.58	0.31	9.70E-10
OPRL1	NO	NO	NO	0.7	0.0025	0.31	1.00E-09
ITGB4	UP	YES	YES	0.35	0.97	0.3	3.70E-08
FOXRED2	UP	YES	YES	0.45	0.1	0.3	5.60E-09
CARD14	NO	NO	NO	0.19	0.14	0.3	5.70E-09
BAIAP2L2	NO	NO	NO	0.17	0.03	0.3	3.60E-09
MDK	UP	YES	YES	0.18	0.19	0.3	2.70E-09
ARHGEF17	NO	NO	NO	0.58	0.24	0.29	8.00E-09
MAPK12	NO	NO	NO	0.48	0.027	0.28	5.10E-08
ERBB3	NO	NO	NO	0.0016	0.0058	0.28	6.80E-08
AGRN	NO	NO	NO	0.011	0.003	0.28	5.90E-08
TAPBP	NO	NO	NO	0.5	0.38	0.27	1.60E-07
SLC6A9	NO	NO	NO	0.31	0.58	0.27	1.40E-07
HVCN1	NO	NO	NO	0.16	0.81	0.27	1.80E-07
GRHPR	NO	NO	NO	0.74	0.31	0.27	1.30E-07
GNG2	NO	NO	NO	0.54	0.54	0.27	1.30E-07
ADGRG1	NO	NO	NO	0.68	0.2	0.27	1.60E-07
MCAM	UP	YES	YES	0.19	0.062	0.26	3.20E-07
MAPK8IP2	NO	NO	NO	0.47	0.45	0.26	4.5-07
IQCK	NO	NO	NO	0.8	0.57	0.26	2.80E-07
ADORA2A	NO	NO	NO	0.8	0.84	0.26	6.3-07
TMC8	NO	NO	NO	0.032	0.36	0.25	1.00E-06
SYNGR4	NO	NO	NO	0.17	0.012	0.25	1.40E-06
CD8A	NO	NO	NO	0.087	0.079	0.25	1.40E-06
AHNAK2	NO	NO	NO	1	0.51	0.25	1.30E-06
WNK2	NO	NO	NO	0.84	0.32	0.24	4.50E-06
VIL1	UP	YES	YES	0.85	0.7	0.24	3.50E-06

TTLL6	NO	NO	NO	0.041	0.23	0.24	3.80E-06
SLC44A2	NO	NO	NO	0.53	0.93	0.24	4.20E-06
RNF224	NO	NO	NO	0.89	0.94	0.24	1.90E-06
RNF223	NO	NO	NO	/	/	0.24	2.40E-06
ACSS1	NO	NO	NO	0.7	0.084	0.23	1.10E-05
ZC3H6	NO	NO	NO	0.73	0.82	0.22	1.60E-05
TRIM7	NO	NO	NO	0.31	0.059	0.22	1.70E-05
STMN3	NO	NO	NO	0.23	0.83	0.22	2.10E-05
LLGL2	NO	NO	NO	0.13	0.7	0.22	1.5-05
CLIC3	NO	NO	NO	0.38	0.35	0.22	2.70E-05
QRICH2	NO	NO	NO	0.096	0.55	0.21	4.30E-05
MST1R	NO	NO	NO	0.026	0.038	0.21	6.20E-05
MN1	NO	NO	NO	0.61	0.82	0.21	5.20E-05
MAPK11	NO	NO	NO	0.49	0.72	0.21	7.10E-05
ABCA2	NO	NO	NO	0.026	0.14	0.21	4.10E-05
SPON2	UP	YES	YES	0.77	0.027	0.2	0.00014
MUC5B	NO	NO	NO	0.42	0.45	0.2	0.00012
MCF2L	NO	NO	NO	0.65	0.18	0.2	0.00011
FGFR3	NO	NO	NO	0.33	0.94	0.2	8.30E-05
ZNF385C	NO	NO	NO	0.21	0.4	0.19	0.00032
ZNF219	NO	NO	NO	0.12	0.74	0.19	0.00027
PRPH	NO	NO	NO	0.56	0.45	0.19	0.00028
PCDH1	NO	NO	NO	0.18	0.05	0.19	0.00029
HR	NO	NO	NO	0.64	0.28	0.19	0.00027
HES4	NO	NO	NO	0.41	0.034	0.19	0.00021
DOK7	NO	NO	NO	0.55	0.2	0.19	0.00028
STAT6	NO	NO	NO	0.97	0.66	0.18	0.00055
SH2D6	NO	NO	NO	0.75	0.03	0.18	0.00037
RAB3D	NO	NO	NO	0.79	0.44	0.18	0.00036
JAG2	NO	NO	NO	0.77	0.89	0.18	0.00037
ETV4	UP	YES	YES	0.22	0.0024	0.18	6.00E-04
CRIP1	UP	YES	YES	0.58	0.56	0.18	0.00038
ACE	NO	NO	NO	0.94	0.72	0.18	0.00051
RASAL1	NO	NO	NO	0.71	0.42	0.17	0.0014
PITPNM3	NO	NO	NO	0.22	0.41	0.17	0.0012
VWA7	NO	NO	NO	0.069	0.13	0.16	0.0016
NTSR1	NO	NO	NO	0.68	0.21	0.16	0.0017
NEURL3	NO	NO	NO	0.029	0.28	0.16	0.0018
GDPD3	NO	NO	NO	0.51	0.2	0.16	0.002
BEST4	NO	NO	NO	0.038	0.78	0.16	0.0027
PPL	NO	NO	NO	0.71	0.24	0.15	0.0048
PIGZ	NO	NO	NO	0.058	0.017	0.15	0.0032
KLHDC8B	NO	NO	NO	0.22	0.014	0.15	0.003
INHBE	NO	NO	NO	0.91	0.53	0.14	0.0055

FSCN2	NO	NO	NO	0.088	0.38	0.14	0.00084
FAM83E	NO	NO	NO	0.71	0.65	0.14	0.0057
AIFM3	NO	NO	NO	0.37	0.49	0.14	0.0084
ADAP1	NO	NO	NO	0.59	0.45	0.14	0.0063
PSCA	NO	NO	NO	0.16	0.035	0.13	0.014
KCNQ1	NO	NO	NO	0.83	0.12	0.13	0.011
CAPS	NO	NO	NO	0.13	0.6	0.13	0.014
VGF	NO	NO	NO	0.89	0.27	0.12	0.018
SEMA3B	NO	NO	NO	0.38	0.21	0.12	0.023
RAC3	UP	YES	YES	0.026	0.15	0.11	0.03
PECAM1	UP	YES	YES	0.66	0.77	0.11	0.043
LBX1	NO	NO	NO	/	/	0.11	0.032
HSD3B7	NO	NO	NO	0.38	0.37	0.11	0.04
GSTP1	NO	NO	NO	0.029	0.97	0.11	0.041
SPOCK2	NO	NO	NO	0.094	0.17	0.1	0.052
GDF15	UP	YES	YES	0.6	0.072	0.1	0.046
FAM20C	NO	NO	NO	0.31	0.84	0.1	0.044
AIF1L	NO	NO	NO	0.069	0.25	0.1	0.049
ISYNA1	NO	NO	NO	0.56	0.41	0.1	0.051
SYT17	NO	NO	NO	0.73	0.15	0.099	0.058
BRSK2	NO	NO	NO	0.2	0.033	0.098	0.06
EFNA2	NO	NO	NO	0.15	0.72	0.097	0.063
NPDC1	NO	NO	NO	0.16	0.79	0.092	0.078
ADSSL1	NO	NO	NO	0.0042	0.025	0.092	0.076
ARHGEF16	NO	NO	NO	0.12	0.021	0.091	0.082
SSTR5	NO	NO	NO	/	/	0.086	0.1
BCAS3	NO	NO	NO	0.87	0.97	0.082	0.11
TJP3	NO	NO	NO	0.67	0.48	0.078	0.13
LRRC75B	NO	NO	NO	0.099	0.87	0.077	0.14
FAS	NO	NO	NO	0.72	0.25	0.076	0.15
S100A14	NO	NO	NO	0.58	0.26	0.073	0.16
RAB37	NO	NO	NO	0.13	0.97	0.068	0.19
TLX1	NO	NO	NO	0.013	0.68	0.067	0.2
MYOM3	NO	NO	NO	0.96	0.47	0.063	0.23
ACTL8	NO	NO	NO	0.85	0.071	0.061	0.25
NPB	NO	NO	NO	0.72	0.18	0.06	0.25
MUC5AC	NO	NO	NO	/	/	0.056	0.28
MGAT4B	NO	NO	NO	0.048	0.0045	0.056	0.29
CRAT	NO	NO	NO	0.66	0.24	0.056	0.28
FKBP5	NO	NO	NO	0.77	0.92	0.055	0.29
NGEF	NO	NO	NO	0.65	0.76	0.054	0.3
IGF2	DOWN	YES	YES	0.29	0.041	0.051	0.33
GIP	NO	NO	NO	/	/	0.049	0.35
SNCG	UP	YES	YES	0.5	0.21	0.048	0.36

FN3K	UP	YES	YES	0.92	0.57	0.047	0.37
PDLIM2	NO	NO	NO	0.42	0.81	0.045	0.39
PRSS36	NO	NO	NO	0.79	0.82	0.041	0.44
PALM	NO	NO	NO	0.94	0.24	0.036	0.49
EGFL7	NO	NO	NO	0.24	0.77	0.035	0.51
GGT1	NO	NO	NO	0.15	0.049	0.034	0.51
OTOF	NO	NO	NO	0.56	0.16	0.032	0.54
CST3	NO	NO	NO	0.58	0.12	0.032	0.54
SLC2A10	NO	NO	NO	0.78	0.93	0.027	0.61
GLI2	NO	NO	NO	0.51	0.38	0.024	0.65
SCNN1D	NO	NO	NO	0.077	0.58	0.023	0.66
ITGA7	NO	NO	NO	0.43	0.15	0.018	0.73
COMTD1	NO	NO	NO	0.87	0.4	0.018	0.74
DBNDD1	UP	YES	YES	0.86	0.32	0.017	0.74
TMPRSS9	NO	NO	NO	0.37	0.88	0.014	0.78
TMEM105	NO	NO	NO	0.58	1	0.013	0.8
RGS11	NO	NO	NO	0.18	0.18	0.013	0.81
FBXL16	NO	NO	NO	0.89	0.84	0.0082	0.88
CHDH	NO	NO	NO	0.72	0.61	0.0016	0.98
SEMA4G	NO	NO	NO	0.94	0.5	0.00092	0.99
PTGDS	NO	NO	NO	0.089	0.67	-0.0051	0.92
ALPI	NO	NO	NO	0.47	0.23	-0.0071	0.89
SPTBN2	DOWN	YES	YES	0.72	0.24	-0.0086	0.87
PANX2	NO	NO	NO	0.81	0.26	-0.013	0.8
TSPAN10	NO	NO	NO	0.81	0.99	-0.013	0.8
TPSG1	NO	NO	NO	0.57	0.25	-0.014	0.79
CPLX1	NO	NO	NO	0.21	0.16	-0.016	0.76
ADAMTSL2	DOWN	YES	YES	0.0026	0.063	-0.016	0.75
KLHDC2	NO	NO	NO	0.79	0.52	-0.018	0.73
SLC25A10	NO	NO	NO	0.86	0.54	-0.027	0.6
NPW	NO	NO	NO	0.55	0.68	-0.035	0.51
CDHR2	DOWN	YES	YES	0.38	0.26	-0.035	0.51
AMN	DOWN	YES	YES	0.52	0.93	-0.035	0.5
MYO7A	DOWN	YES	YES	0.43	0.89	-0.036	0.49
SLC22A18AS	NO	NO	NO	0.62	0.38	-0.072	0.17
RAB26	NO	NO	NO	0.73	0.42	-0.083	0.11
SDC1	NO	NO	NO	0.64	0.54	-0.086	0.099
PNPLA7	DOWN	YES	YES	0.61	0.15	-0.091	0.081
NR0B2	NO	NO	NO	0.37	0.21	-0.094	0.072
EEF1A2	UP	YES	YES	0.011	0.56	-0.097	0.062
PLCH2	DOWN	YES	YES	0.35	0.69	-0.1	0.048
TNXB	NO	NO	NO	0.046	0.58	-0.12	0.027
MLXIPL	DOWN	YES	YES	0.98	0.023	-0.12	0.017
NDRG2	DOWN	YES	YES	0.14	0.064	-0.13	0.014

NUDT8	NO	NO	NO	0.59	0.76	-0.14	0.0066
SLC22A18	NO	NO	NO	0.3	0.57	-0.18	0.00052
REEP6	NO	NO	NO	0.4	0.91	-0.18	0.00071
GCGR	DOWN	YES	YES	0.15	0.044	-0.18	0.00046
F7	NO	NO	NO	0.0086	0.14	-0.18	0.00043
RARRES2	NO	NO	NO	0.8	0.9	-0.2	0.00011
LIMS2	NO	NO	NO	0.034	0.0048	-0.2	7.50E-05
GLTPD2	NO	NO	NO	0.015	0.22	-0.2	0.00012
FBP1	DOWN	YES	YES	0.013	0.12	-0.21	4.40E-05
COL18A1	NO	NO	NO	0.079	0.006	-0.26	3.30E-07
GAMT	NO	NO	NO	0.13	0.23	-0.27	2.30E-07
C8G	NO	NO	NO	0.7	0.49	-0.29	9.00E-09
BTD	NO	NO	NO	0.85	0.28	-0.15	0.0045
TNNC2	NO	NO	NO	0.37	0.72	-0.085	0.1
PKD2L1	NO	NO	NO	0.3	0.47	-0.011	0.84
TOGARAM2	/	/	/	/	/	/	/
SNORC	/	/	/	/	/	/	/
PLPPR2	/	/	/	/	/	/	/
LOC105373989	/	/	/	/	/	/	/
CBARP	/	/	/	/	/	/	/
CATSPERZ	/	/	/	/	/	/	/
C10orf143	/	/	/	/	/	/	/
ATP5F1D	/	/	/	/	/	/	/

HCC, hepatocellular carcinoma; GEPIA, gene expression profile interactive analysis

Table S8. Correlation analysis of *KIF2C, MYBL2, HMGB2, AURKA* expression and Nucleus, Cytoplasm *ANLN* in HCC, respectively.

Substance		Nucleus *ANLN*		P value#	Cytoplasm *ANLN*		P value#
		High(N=132)	Low(N=133)		High(N=132)	Low(N=133)	
KIF2C	High(N=132)	85	47	<0.001	59	73	0.097
	Low(N=133)	57	88		73	60	
MYBL2	High(N=132)	81	50	<0.001	62	69	0.424
	Low(N=133)	51	83		70	64	
HMGB2	High(N=132)	77	56	<0.001	64	69	0.581
	Low(N=133)	55	77		68	64	
AURKA	High(N=132)	75	57	<0.001	60	72	0.158
	Low(N=133)	57	76		72	61	

#Note：the $\chi 2$ test was used for comparison between groups.

Table S9. Antibodies and dilutions used in this study.

Cat. No	Antibody	Species	Dilution	Company	Application
ab195352	Mettl3	Rabbit	1:1000	Abcam	WB
ab220162	YTHDF1	Rabbit	1:1000	Abcam	WB
A6524	ANLN	Rabbit	1:1000	Abclonal	WB
ab231778	SP1	Rabbit	1:1000	Abcam	WB
ab215206	FOXP3	Rabbit	1:1000	Abcam	WB
AP0115	S2448P-mTOR	Rabbit	1:1000	Abclonal	WB
A2445	mTOR	Rabbit	1:1000	Abclonal	WB
ab32572	β-Catentin	Rabbit	1:1000	Abcam	WB
AF5131	VEGFA	Rabbit	1:1000	Affinity	WB
AF6294	STAT3	Rabbit	1:1000	Affinity	WB
AF3293	Phospho (Tyr705)-STAT3	Rabbit	1:1000	Affinity	WB
AF6432	4E-BP1	Rabbit	1:1000	Affinity	WB
AF3432	Phospho-4E-BP1 (Thr45)	Rabbit	1:1000	Affinity	WB
AF6226	S6K1	Rabbit	1:1000	Affinity	WB
AF3228	p70 (Thr389/Thr412)-S6K1	Rabbit	1:1000	Affinity	WB
A16909	Lamin B1	Rabbit	1:1000	Abclonal	WB
ab52866	α-Tubulin	Rabbit	1:1000	Abcam	WB
A5449	KIF2C	Rabbit	1:1000	Abclonal	WB
MABE886	MYBL2	Mouse	1 μg/mL	Sigma-Aldrich	WB
A9168	HMGB2	Rabbit	1:1000	Abclonal	WB
A15728	AURKA	Rabbit	1:1000	Abclonal	WB
ab8226	ACTIN	Mouse	1:10000	Abclonal	WB
ab6721	Goat Anti-Rabbit IgG H&L (HRP)	Goat	1:10000	Abcam	WB
ab6789	Goat Anti-Mouse IgG H&L (HRP)	Goat	1:10000	Abcam	WB
DF12020	Mettl3	Rabbit	1:50	Affinity	IHC
17479-1-AP	YTHDF1	Rabbit	1:50	proteintech	IHC
DF13590	ANLN	Rabbit	1:50	Affinity	IHC
A5449	KIF2C	Rabbit	1:50	Abclonal	IHC
DF7817	MYBL2	Rabbit	1:50	Affinity	IHC
A9168	HMGB2	Rabbit	1:50	Abclonal	IHC
A15728	AURKA	Rabbit	1:50	Abclonal	IHC
A17924	N6-methyladenosine / m6A Rabbit pAb	Rabbit	1:50	Abclonal	IP, RIP, and ChIP
AE063	anti-FLAG	Rabbit	1:50	Abclonal	IP, RIP, and ChIP
A6524	ANLN	Rabbit	1:50	Abclonal	IP, RIP, and ChIP
ab215206	FOXP3	Rabbit	1:30	Abcam	IP, RIP, and ChIP
ab231778	SP1	Rabbit	1:30	Abcam	IP, RIP, and ChIP
AE012	anti-GFP	Mouse	1:50	Abclonal	IP, RIP, and ChIP
ab205718	Goat Anti-Rabbit IgG H&L (HRP)	Goat	1:50	Abcam	IP, RIP, and ChIP
ab6789	Goat Anti-Mouse IgG H&L (HRP)	Goat	1:50	Abcam	IP, RIP, and ChIP
ab32572	β-Catentin	Rabbit	1:50	Abcam	IF
ab7090	Goat Anti-Rabbit IgG H&L (HRP)	Goat	1:50	Abcam	IF

WB, western blot; IHC, immunohistochemistry

Table S10. Primer sequences for plasmid construction

Gene Name	sequence (5'-3')
Mettl3-KD#1	GCAAGAATTCTGTGACTATGG
Mettl3-KD#1	GCTGCACTTCAGACGAATTAT
Mettl3-KD#1	GCTACCTGGACGTCAGTATCT
YTHDF1-KD#1	GGATACAGTTCATGACAATGA
YTHDF1-KD#2	GCACTGACTGGTGTCCTTTCT
YTHDF1-KD#3	GGAAACGTCCAGCCTAATTCT
ANLN-KD#1	GGTGGTGAAGAGAAATCTTGT
ANLN-KD#2	GCAGATACCATCAGTGATTCT
ANLN-KD#3	GCTACATTCTGTTCCCAAAGG
MYBL2-KD#1	GCCATGGACCAAAGAGGAAGA
MYBL2-KD#2	GGACAGACAATGCTGTGAAGA
MYBL2-KD#3	GCCCAAGAGCACACCTGTTAA
AURKA-KD#1	GGACCTGTTAAGGCTACAGCT
AURKA-KD#2	GGGTCTTGTGTCCTTCAAATT
AURKA-KD#3	GGGCTTTGGAAGACTTTGAAA
HMGB2-KD#1	GGAGGAGGAAGAAGAAGATGA
HMGB2-KD#2	GCGGAATTCTCCAAGAAGTGT
HMGB2-KD#3	GCTAAGCTAAAGGAGAAATAT
KIF2C-KD#1	GCAGTGGCTGAAATACCATTG
KIF2C-KD#2	GGAAATCATGTCTTGTGAAGG
KIF2C-KD#3	GCAAGAATTGGCCAAGAAAGA
Control-KD	TTCTCCGAACGTGTCACGT

KD. knock down

Table S11. Primers for real-time PCR listed used in this study.

Name	Sequence
METTL3-F	TTGTCTCCAACCTTCCGTAGT
METTL3-R	CCAGATCAGAGAGGTGGTGTAG
METTL14-F	GAACACAGAGCTTAAATCCCCA
METTL14-R	TGTCAGCTAAACCTACATCCCTG
WTAP-F	TTGTAATGCGACTAGCAACCAA
WTAP-R	GCTGGGTCTACCATTGTTGATCT
KIAA1429-F	TACTTTGAGCCCATTTCTCCTGA
KIAA1429-R	GGAATACTGTCTACTGTTCGTCG
ALKBH5-F	CGGCGAAGGCTACACTTACG
ALKBH5-R	CCACCAGCTTTTGGATCACCA
FTO-F	ACTTGGCTCCCTTATCTGACC
FTO-R	TGTGCAGTGTGAGAAAGGCTT
YTHDF1-F	ATACCTCACCACCTACGGACA
YTHDF1-R	GTGCTGATAGATGTTGTTCCCC
YTHDF2-F	CCTTAGGTGGAGCCATGATTG
YTHDF2-R	TCTGTGCTACCCAACTTCAGT
YTHDF3-F	TCAGAGTAACAGCTATCCACCA
YTHDF3-R	GGTTGTCAGATATGGCATAGGCT
ANLN-F	ATCTTGCTGCAACTATTTGCTCC
ANLN-R	TCCTGCTTAACACTGCTGCTA
CENPA-F	TTCCTCCCATCAACACAGTCG
CENPA-R	CACACCACGAGTGAATTTAACAC
KIF2C-F	CTGTTTCCCGGTCTCGCTATC
KIF2C-R	AGAAGCTGTAAGAGTTCTGGGT
PRR11-F	GACTTCCAAAGCTGTGC TTCC
PRR11-R	CTGCATGGGTCCATCC TTTTT
DLGAP5-F	AAGTGGGTCGTTATAGACCTGA
DLGAP5-R	TGCTCGAACATCACTCTCGTTAT
PHF19-F	ACTCGGGACTCCTATGGTGC
PHF19-R	CCTCCGTCAGTTTGGACATCA
BIRC5-F	AGGACCACCGCATCTCTACAT
BIRC5-R	AAGTCTGGCTCGTTCTCAGTG
MYBL2-F	GAGGGATAGCAAGTGCAAGGT
MYBL2-R	TGCGGTTAGGGAAGTGGCTG
CDCA5-F	GACGCCAGAGACTTGGAAATG
CDCA5-R	GGACCTCGGTGAGTTTGGAG
HMGB2-F	GTGGCCTAGCTCGTCAAGTT
HMGB2-R	GCGTACGAGGACATTTTGCC
TACC3-F	TCGCCACCAGAAGTTACCG
TACC3-R	TCCCGCAGAGGTGTCTGAAA
FAM83D-F	GGGAAGGTTCACGAAAAGTTCA
FAM83D-R	GACTGGGCATACAGGATTCGG

IQGAP3-F	GCAGCCTATGAACGCCTCA
IQGAP3-R	GGAGGGTGCAAAACAGTGG
AURKA-F	CAGACTGGATACCGGGACC
AURKA-R	CTTCAGCACGTTTTTGCACTG
VEGFA-F	AGGGCAGAATCATCACGAAGT
VEGFA-R	AGGGTCTCGATTGGATGGCA
RANKL-F	CATGTTCGTGGCCCTCCTG
RANKL-R	CATGTTCGTGGCCCTCCTG
RANK-F	CCGCCTAAGTGGAGATAAGGAAA
RANK-R	CGTAGACCACGATGATGTCGC
ACTIN-F	TGGCACCCAGCACAATGAA
ACTIN-R	CTAAGTCATAGTCCGCCTAGAAGCA

Supplementary References

[1] Yuan JH, Yang F, Wang F. *et al*. A long noncoding RNA activated by TGF-β promotes the invasion-metastasis cascade in hepatocellular carcinoma. Cancer Cell 2014; 25:666-681.

[2] Petroski MD, Deshaies RJ. Function and regulation of cullin-RING ubiquitin ligases. Nat Rev Mol Cell Biol 2005; 6:9-20.

[3] Dominissini D, Moshitch-Moshkovitz S, Salmon-Divon M. *et al*. Transcriptome-wide mapping of N (6)-methyladenosine by m (6)A-seq based on immunocapturing and massively parallel sequencing. Nat Protoc 2013; 8:176-189.

[4] Shen C, Sheng Y, Zhu AC. *et al*. RNA Demethylase ALKBH5 Selectively Promotes Tumorigenesis and Cancer Stem Cell Self-Renewal in Acute Myeloid Leukemia. Cell Stem Cell 2020; 27:64-80. e9.

[5] Li C, Wang S, Xing Z. *et al*. A ROR1-HER3-lncRNA signalling axis modulates the Hippo-YAP pathway to regulate bone metastasis. Nat Cell Biol 2017; 19:106-119.

[6] Sun W, Li SC, Xu L. *et al*. High FLT3 Levels May Predict Sorafenib Benefit in Hepatocellular Carcinoma. Clin Cancer Res. 2020;15;26(16):4302-4312.